

NASA CR-122446

DEVELOPMENT OF IMPROVED PYROELECTRIC DETECTORS

Measurements of pyroelectric material characteristics and FET characteristics

Seymour Weiner and Henry P. Beerman

Barnes Engineering Company, Inc.

30 Commerce Road

Stamford, Conn. 06904

Reproduced by
NATIONAL TECHNICAL
INFORMATION SERVICE
U S Department of Commerce
Springfield VA 22151

June 30, 1972

Quarterly Technical Report for Period February 1972 - May 1972

Prepared for

GODDARD SPACE FLIGHT CENTER

Greenbelt, Maryland 20771



N72-28456
Unclas
35405
CSSL 14B G3/14
DEVELOPMENT OF IMPROVED
PYROELECTRIC DETECTORS: MEASUREMENTS OF
PYROELECTRIC MATERIAL CHARACTERISTICS AND
FET S. Weiner, et al (Barnes Engineering
Co.) 28 Jul. 1972 65 p

NATIONAL AERONAUTICS AND SPACE ADMINISTRATION

1. Report No.	2. Government Accession No.	3. Recipient's Catalog No.	
4. Title and Subtitle Development of Improved Pyroelectric Detectors		5. Report Date June 30, 1972	6. Performing Organization Code
7. Author(s) Seymour Weiner, Henry Beerman		8. Performing Organization Report No. BEC 2064QR 3	
9. Performing Organization Name and Address Barnes Engineering Company 30 Commerce Rd. Stamford, Conn. 06904		10. Work Unit No.	11. Contract or Grant No. NAS5-21655
12. Sponsoring Agency Name and Address National Aeronautics & Space Administration Goddard Space Flight Center Greenbelt, Maryland 20771		13. Type of Report and Period Covered Quarterly Technical Feb. 23, 1972 to May 22, 1972	
14. Sponsoring Agency Code			
15. Supplementary Notes Andrew W. McCulloch, Code 652, Tech. Monitor			
16. Abstract <p>The object of this program is to improve the detectivity of the pyroelectric detector with the ultimate goal of operation at or near the temperature-noise limit. Two general areas of investigation are undertaken. The first is to improve responsivity through the use of new materials. The second is directed toward reduction of noise and will be effected with improved field effect transistor characteristics, and improved electroding of the pyroelectric material.</p> <p>The review of the literature on pyroelectric materials continues. From this, several materials have already been selected for investigation, and several were tested.</p> <p>FET's are being obtained from various manufacturers, evaluated, and selected units tested for evaluation of characteristics critical to their use as preamplifiers with pyroelectric detectors.</p>			
17. Key Words (Selected by Author(s)) Infrared Detectors Pyroelectricity Ferroelectricity		18. Distribution Statement	
19. Security Classif. (of this report) Unclassified	20. Security Classif. (of this page) Unclassified	21. No. of Pages 64	22. Price* 5.25

PREFACE

The object of this program is to improve the detectivity of the pyroelectric detector with the ultimate goal of operation at or near the temperature-noise limit.

During the third phase of this program efforts were concentrated on completing measurements of the pyroelectric coefficient, dielectric constant, and loss-tangent as a function of temperature for the most promising detector materials. This data is now complete over a temperature range from -30°C to approximately 100°C for the following 10 materials: TGS; DTGS; gamma-irradiated TGS, gamma-irradiated DTGS, gamma-irradiated TGFB; $\text{Li}_2\text{SO}_4 \cdot \text{H}_2\text{O}$; $\text{Sr}_{0.75}\text{Ba}_{0.25}\text{Nb}_2\text{O}_6$; $(\text{Li}_2\text{O})_{0.49}(\text{Ta}_2\text{O}_5)_{0.51}$; Gulton PZT-G1306; and Honeywell 4/60/40 PLZT. Additional pyroelectric coefficient measurements only are included for TGFB, $\text{TGS}_{0.88}\text{TGFB}_{0.12}$, and ethylene diamine tartrate (EDT).

Fully poled TGS, DTGS, TGFB, subsequently gamma-irradiated from a cobalt '60' source, was shown to have "locked-in" polarization. Using DL- α -alanine to dope a DTGS crystal during growth below the Curie temperature, it was subsequently confirmed that "locked-in" polarization is similarly achieved. However, the presence of both D & L components of α -alanine leads to erratic behavior of the pyroelectric coefficient as a function of temperature. Use of only the L- α -alanine as a dopant apparently leads to satisfactory performance according to preliminary data obtained from a small crystal sample.

Spectral data (transmittance and reflectance from 0.25 to 40μ) was obtained for ethylene diamine tartrate (EDT), most of the other materials having been reported in the two previous quarterly reports.

All new available data has been incorporated in a revised table of pyroelectric materials characteristics and included in this report.

The low noise preamplifier and post amplifier, for evaluating completed detectors made from the most promising pyroelectric materials, has been completed.

Project accomplishments are consistent with the objectives of the program.

TABLE OF CONTENTS

1.0 INTRODUCTION 1-1

2.0 LITERATURE SEARCH..... 2-1

3.0 MEASUREMENTS..... 3-1

 3.1 TRANSMITTANCE AND REFLECTANCE..... 3-1

 3.2 PYROELECTRIC COEFFICIENT, DIELECTRIC CONSTANT,
 AND LOSS TANGENT..... 3-1

 3.3 DETECTOR RESPONSIVITY AND NOISE MEASUREMENT..... 3-6

4.0 NEW TECHNOLOGY..... 4-1

5.0 PLANNED FOR NEXT REPORT PERIOD..... 5-1

6.0 CONCLUSION AND RECOMMENDATIONS..... 6-1

APPENDICES

A. COMPILATION OF PYROELECTRIC MATERIALS AND THEIR
 CHARACTERISTICS..... A-1

B. MEASURED DATA ON SELECTED PYROELECTRIC MATERIALS:
 OPTICAL TRANSMISSION, OPTICAL REFLECTANCE..... B-1

C. PYROELECTRIC COEFFICIENT, DIELECTRIC CONSTANT, AND
 LOSS TANGENT CURVES OF SELECTED PYROELECTRIC MATERIALS.... C-1

REFERENCES

LIST OF ILLUSTRATIONS

- C1-a PYROELECTRIC COEFFICIENT OF TGS VS. TEMPERATURE
- C1-b DIELECTRIC CONSTANT OF TGS VS. TEMPERATURE
- C1-c LOSS TANGENT OF TGS VS. TEMPERATURE
- C2-a PYROELECTRIC COEFFICIENT OF GAMMA IRRADIATED TGS VS. TEMPERATURE
- C2-b DIELECTRIC CONSTANT OF GAMMA IRRADIATED TGS VS. TEMPERATURE
- C2-c LOSS TANGENT OF GAMMA IRRADIATED TGS VS. TEMPERATURE
- C3-a PYROELECTRIC COEFFICIENT OF DTGS VS. TEMPERATURE
- C3-b DIELECTRIC CONSTANT OF DTGS VS. TEMPERATURE
- C3-c LOSS TANGENT OF DTGS VS. TEMPERATURE
- C4-a PYROELECTRIC COEFFICIENT OF GAMMA IRRADIATED DTGS VS. TEMPERATURE
- C4-b DIELECTRIC CONSTANT OF GAMMA IRRADIATED DTGS VS. TEMPERATURE
- C4-c LOSS TANGENT OF GAMMA IRRADIATED DTGS VS. TEMPERATURE
- C5-a PYROELECTRIC COEFFICIENT OF TGFB VS. TEMPERATURE
- C6-a PYROELECTRIC COEFFICIENT OF GAMMA IRRADIATED TGFB VS. TEMPERATURE
- C6-b DIELECTRIC CONSTANT OF GAMMA IRRADIATED TGFB VS. TEMPERATURE
- C6-c LOSS TANGENT OF GAMMA IRRADIATED TGFB VS. TEMPERATURE
- C7-a PYROELECTRIC COEFFICIENT OF $\text{TGS}_{0.88}\text{TGFB}_{0.12}$ VS. TEMPERATURE
- C8-a PYROELECTRIC COEFFICIENT OF $\text{Li}_2\text{SO}_4\text{H}_2\text{O}$ VS. TEMPERATURE
- C8-b DIELECTRIC CONSTANT AND LOSS TANGENT OF $\text{Li}_2\text{SO}_4\text{H}_2\text{O}$ VS. TEMPERATURE
- C9-a PYROELECTRIC COEFFICIENT OF $\text{Sr}_{1-.25}\text{Ba}_{.25}\text{Nb}_2\text{O}_6$ VS. TEMPERATURE
- C9-b DIELECTRIC CONSTANT OF $\text{Sr}_{1-.25}\text{Ba}_{.25}\text{Nb}_2\text{O}_6$ VS. TEMPERATURE
- C9-c LOSS TANGENT OF $\text{Sr}_{1-.25}\text{Ba}_{.25}\text{Nb}_2\text{O}_6$ VS. TEMPERATURE
- C10-a PYROELECTRIC COEFFICIENT OF $(\text{Li}_2\text{O})_{0.49}(\text{Ta}_2\text{O}_5)_{0.51}$ VS. TEMPERATURE
- C10-b DIELECTRIC CONSTANT AND LOSS TANGENT OF $(\text{Li}_2\text{O})_{0.49}(\text{Ta}_2\text{O}_5)_{0.51}$ VS. TEMP.
- C11-a PYROELECTRIC COEFFICIENT OF GULTON PZT G-1306 VS. TEMPERATURE
- C11-b DIELECTRIC CONSTANT OF GULTON PZT G-1306 VS. TEMPERATURE
- C11-c LOSS TANGENT OF GULTON PZT G-1306 VS. TEMPERATURE
- C12-a PYROELECTRIC COEFFICIENT OF HONEYWELL 4/60/40 PLZT VS. TEMPERATURE
- C12-b DIELECTRIC CONSTANT OF HONEYWELL 4/60/40 PLZT VS. TEMPERATURE
- C12-c LOSS TANGENT OF HONEYWELL 4/60/40 PLZT VS. TEMPERATURE
- C13-a PYROELECTRIC COEFFICIENT OF ETHYLENE DIAMINE TARTRATE VS. TEMPERATURE

Section 1.0 INTRODUCTION

The third phase of this program has been carried out over a three month period beginning February 23, 1972 and ending May 26, 1972.

The goals of the third phase were as follows:

1. Continue the literature search for new pyroelectric materials and update the compiled data started in the first phase.
2. Continue the transmittance and reflectance measurements of those samples not previously measured.
3. Measure the dielectric constant and loss tangent as a function of temperature (-30°C to approximately 100°C) and frequency (50 Hz to 10 KHz) for all samples on hand. Similarly, measure the pyroelectric coefficient as a function of temperature.
4. Investigate gamma-irradiated TGS, DTGS, and α -alanine doped TGS and DTGS as a means of achieving "locked-in" polarization.
5. Fabricate $1.5 \times 1.5 \times 0.04$ mm detector samples from the most promising detector materials, and mate them to the best available transistors. Measure responsivity, noise, detectivity, and spectral response of the evacuated devices as functions of temperature and frequency.
6. Grow a crystal of glucuronolactone from an aqueous solution.
7. Time permitting, examine the effects of U.V. radiation on TGS and DTGS to obtain locked-in polarization.
8. Continue the search for improved FET's and determine their characteristics along with the best mode of operation of the detector-amplifier package.
9. Operate a SBN detector in the dielectric mode and record its performance.

Due to reduced funding of the entire program, priorities had to be established to achieve the most important results during the reporting period.

The goals listed above under 1, 2, 3, 4, and 8 were achieved and are each discussed in turn in the remainder of this report. Difficulties that arose, causing delays in some goals, are also discussed. It is hoped that subsequent funding will permit completion of the intended goals.

Section 2.0 LITERATURE SEARCH

The literature search for pyroelectric materials and their parameters has been carried forward on a continual basis and the table of pyroelectric materials characteristics updated. The references to ferroelectrics and pyroelectrics are ever-growing. Some of the more pertinent papers that were encountered during the reporting period are herewith cited.

Since the work by Lock (L5) in obtaining locked-in polarization by using α -alanine doped TGS was reported in the second quarterly report, further reports on this phenomenon have become available through Keve et al. (K5, K6). Introduction of optically active L- α -alanine into a TGS crystal causes an asymmetric distorted glycine I (Hoshino, H7) molecule. Each optically active L- α -alanine molecule has its α -CH₃ group pointing in the same direction with respect to the b axis of TGS. The resultant dipoles have the same polar sense and will result in a self bias. Other suggested dopants are serine, and α -amino-n-butyric acid. DL- α -alanine is reported to give similar effects to L- α -alanine as long as the TGS is grown below the Curie temperature. L- α -alanine doped TGS (LATGS) yields a fully poled pyroelectric detector with reduced losses, resulting, according to Lock (L5), in a D^* of 2×10^9 cm-cps^{1/2} w⁻¹ at 10 Hz for a 0.5 x 0.5 mm element.

Haertling and Land (H8) discuss the material processing of lanthanum-doped lead zirconate titanate (PLZT), namely an oxide-alkoxide co-precipitation chemical process, followed ultimately by a hot press in an oxygen atmosphere at 1200°C and 3000 psi for 16 hours. Compositions of 7/65/35, 8/65/35, 2/65/35 and 12/40/60 are discussed, where the ratio stands for La/Zr/Ti. A sample of 4/60/40 PLZT was obtained from Honeywell for evaluation.

Since Yamaka et al (Y4) were reported in the second quarterly report to have achieved a D^* of 8×10^8 cm-cps^{1/2} w⁻¹ for a PbTiO₃ detector, efforts were expended trying to obtain samples and/or literature of PbTiO₃. No domestic commercial producers of PbTiO₃ single crystals were found. However, Bhide et al (B8) describe a method whereby a mixture of TiO₂:Pb₃O₄:KF in the ratio of 1:2.5:6.5, heated to between 900°C and 950°C for 20 hours and followed by slow cooling to room temperature over 16 hours yields 2 x 2 x 0.25 cm single crystals. A dielectric constant of 30 at ambient for 10K Hz is claimed which contrasts sharply with Yamaka's value of 200. While Yamaka does not say so, it is believed that his PbTiO₃ crystal is doped, probably with uranium oxide (UO₃).

Remeika and Glass (R2) have reported data on 0.1% UO₃ doped PbTiO₃. Doping raises the room temperature DC resistivity from 10⁶ ohm-cm (undoped) to 10¹⁰ ohm-cm. They obtained 1 x 3 x 5 mm crystals grown from the melt (including flux) which is kept 5 hours at 1100°C and then allowed to cool to 700°C at a rate of 5°C/hr. Detwinning was accomplished by applying pressure to the platelet edges above 250°C.

McFee et al (M5) obtained an NEP of 1.5×10^{-8} w Hz^{-1/2} for a 19μ-thick polyvinylidene fluoride PVF₂ film at 90 Hz for a 2 mm² detector, which is a factor of 20 worse than for a TGS detector of equivalent area. To pole the material 10⁶ v/cm are applied across the film at 120°C. The film is then allowed to cool to ambient temperature with the field applied. They used the charge integration technique to determine the pyroelectric coefficient. Efforts at BEC to measure the pyroelectric coefficient of PVF₂ and polyvinyl-fluoride (PVF) by the charge integration method were unsuccessful to date due to a high leakage rate even under steady state condition.

Section 3.0 MEASUREMENTS

3.1 Transmittance and Reflectance

The only new pyroelectric material whose transmittance and reflectance was measured from 0.25μ to 40μ during the reporting period was 1 mm thick ethylene diamine tartrate [EDT, $C_2H_4(NH_3)_2C_4H_4O_6$], obtained from the Isomet Corporation. The graphs are found in Appendix B. It proved difficult to obtain a good polished surface on the EDT sample and this may account for the low value of the normal reflectance.

3.2 Pyroelectric Coefficient, Dielectric Constant, and Loss Tangent

The equipment used in measuring respectively the pyroelectric coefficient, and dielectric constant plus loss tangent, are shown in Figure 4-11 and Figure 4.1 of the second quarterly report. All electroded samples were 5 x 5 mm in area and either 1 mm or 0.5 mm in thickness. To date ten materials have a completed set of measurements for pyroelectric coefficient, dielectric constant, and loss tangent over a temperature range from $-30^\circ C$ to approximately $80^\circ C$ and frequencies ranging from 100 Hz to 10K Hz (and in several cases to 100K Hz). They are TGS; DTGS; gamma-irradiated (2.3 MegaRöntgen from a Cobalt ⁶⁰ source) TGS, DTGS, and TGFB; $Li_2SO_4 \cdot H_2O$; $Sr_{0.75}Ba_{0.25}Nb_2O_6$; Gulon PZT G-1306; Honeywell PLZT 4/60/40; and $LiTaO_3$. In addition, only pyroelectric coefficient vs. temperature measurements are complete for TGFB, $TGS_{0.88}TGFB_{0.12}$, and ethylene diamine tartrate (EDT). All graphs pertaining to the pyroelectric coefficient, dielectric constant and loss tangent vs. temperature are found in Appendix C.

A few dielectric constant and loss tangent vs. temperature curves (i.e. TGS, DTGS, and $Li_2SO_4 \cdot H_2O$) have been included previously in the second quarterly report. For completeness they have been included again in this report. The gamma irradiated samples reported on in the second quarterly report were subsequently found to have been incompletely poled prior to gamma irradiation. The

original samples required subsequent additional poling to obtain the maximum pyroelectric coefficient at all temperatures below the Curie temperature. On exceeding the Curie temperature and cooling without repoling, the samples would revert to a lower pyroelectric coefficient. In contrast, the new fully-poled and gamma-irradiated samples of TGS, DTGS, and TGFB yield the maximum pyroelectric coefficient at all temperatures below the Curie temperature without need for additional poling. Fully poled samples yield also a somewhat lower dielectric constant and considerably lower loss tangent.

Consistently better results were obtained when the 5x5x0.5 mm electroded samples of TGS, DTGS, and TGFB were mounted on their respective headers, then poled and gamma irradiated, rather than poling and irradiating a large ($\geq 2 \text{ cm}^2$) electroded 0.5 mm thick slice followed by dicing into 5 x 5 mm elements. Thus, it seems advisable to mount future electroded infrared detector elements of either TGS, DTGS, or TGFB onto their final substrate (eliminating temporarily the FET), followed by poling and irradiation of the individual elements rather than processing elements from poled and irradiated slices.

The previously reported initial curve for the pyroelectric coefficient vs. temperature for TGS (Figure 4-19, second quarterly report) was re-run and a better fit obtained around ambient temperature that eliminates the previous "bump" in the curve (Figure C 1-a). However, a similar bump was obtained in the pyroelectric coefficient vs. temperature curve for gamma-irradiated DTGS around ambient temperature (Figure C 4-a).

$\text{Li}_2\text{SO}_4 \cdot \text{H}_2\text{O}$ was found to exhibit a peak in its pyroelectric coefficient at 70°C (Figure C 8-a). It is questionable that this represents a Curie temperature. Since an irreversible increase in the loss tangent (and dielectric constant) at all temperatures was found whenever the material had been heated to $70\text{-}80^\circ\text{C}$ or higher, it is felt that the peak in the pyroelectric coefficient merely represents the lowest temperature where decomposition begins.

$\text{Li}_2\text{SO}_4 \cdot \text{H}_2\text{O}$ detectors previously made at BEC in past years never lived up to their expected detectivity (as based on published parameters). It appears that this degradation was caused by the excessive bake-out temperature of approximately 80-100°C during evacuation.

Poled SBN ($x=0.25$) from Crystal Technology, Inc., did not give initially repeatable results for the pyroelectric coefficient vs. temperature curve. The sample was kept at 76°C for 16 hours without bias and then it was then cooled rapidly (thermoelectrically) to -30°C without bias. On measuring the pyroelectric coefficient with increasing temperature, repeatable results were obtained (Figure C 9-a). Although no previous external poling was applied to the SBN sample, the pyroelectric coefficient obtained at 25°C ($37 \times 10^{-8} \text{C-cm}^{-2}\text{K}^{-1}$) compares favorably with the value reported by Glass (G4) of $31 \times 10^{-8} \text{C-cm}^{-2}\text{K}^{-1}$. Of interest is the rather marked difference in temperature where the respective pyroelectric coefficient and dielectric constant of SBN ($x=0.25$) reaches a maximum. All Curie temperatures have been reported on the basis of maximum pyroelectric coefficient rather than maximum dielectric constant. Increasing the field strength across any pyroelectric sample will generally shift the temperature at which a maximum dielectric constant is obtained to slightly higher temperatures. Glass (G3) feels that it is not possible to define a Curie temperature for low Ba content SBN crystals because of the broad peaks obtained for the dielectric constant. This implies that the ferroelectric-paraelectric phase transition does not occur at a discrete temperature.

LiTaO_3 (or in this case more precisely $(\text{Li}_2\text{O})_{0.49}\text{Ta}_2\text{O}_5$)_{0.51} from Crystal Technology Inc., was found to have the lowest loss tangent (Figure C 10-b) of all materials encountered so far. Its responsivity and detectivity figures of merit compare favorably with those of TGS, DTGS, and TGFB. The material also exhibits very little change in its pyroelectric parameters with change in temperature

so that its responsivity and detectivity should be rather constant over a wide operating temperature range. For high ambient temperature operation and/or high incident energy levels (lasers), it appears as the most promising detector material.

Comparing Honeywell PLZT 4/60/40 (Figures C 12-a,b,c) with Gulton PZT-G1306 (Figures C 11-a,b,c) - both being polycrystalline ceramic materials - it will be noted that the former has generally a higher pyroelectric coefficient and lower dielectric constant than the latter, so that the responsivities of these particular PLZT and PZT formulations will be in a ratio of $\approx 3:1$. However, the loss tangent of the PLZT is markedly higher than that for PZT so that the expected detectivities are roughly equal.

Due to the low pyroelectric coefficient of EDT (Figure C 13-a), the equipment had to be run at a higher gain than all the other samples. This accentuated the hysteresis effect (difference between pyroelectric coefficient on heating and cooling). Therefore, a mean value was plotted. The value obtained at 20°C ($0.25 \times 10^{-8} \text{ C-cm}^{-2} \text{ }^\circ\text{K}^{-1}$) is in good agreement with one reported by Putley (P1) of $0.2 \times 10^{-8} \text{ C-cm}^{-2} \text{ }^\circ\text{K}^{-1}$.

Attempts were made to measure the pyroelectric coefficient of polyvinyl fluoride (PVF) and polyvinylidene fluoride (PVF₂) films. After electroding, poling, and letting the samples stay at ambient temperature without bias for 24 hours, a continual charge output was obtained even at a constant temperature. This made it impossible to measure dPs/dT . These samples may have been improperly poled. The measurements on PVF and PVF₂ will have to be repeated since both materials are appealing as inexpensive large area infrared detectors where the highest responsivity and detectivity are not required.

Keve et al (K6) point out that TGS doped with a racemic mixture of D and L- α -alanine (DLATGS) and grown below the Curie temperature, generally gave results comparable to L- α -alanine doped TGS. In order to have a higher Curie temperature, a deuterated TGS

crystal doped with racemic D and L- α -alanine was grown over a temperature range from 42.8° to 36.5°C. Judging by the performance of the DL- α -alanine doped DTGS on trying to measure the pyroelectric coefficient with temperature, the material must exhibit a double segmented hysteresis loop (K6-p.44), coming from two or more crystal regions of permanent self bias of opposite sense. No two samples of DLADTGS behaved the same on measuring dPs/dT . One sample exhibited almost no pyroelectric coefficient at ambient temperature, subsequently increasing at higher temperature. Whenever a peak pyroelectric coefficient was obtained, there would be a sudden sign reversal on further increasing the temperature slightly. Peaks obtained with increasing temperature would not agree with peaks obtained with decreasing temperature. Another sample behaved properly above ambient temperature to the Curie temperature but behaved similarly erratic below ambient temperature.

Doping a DTGS crystal with only L- α -alanine was deemed to overcome the problems encountered with a racemic admixture. The present plan is to subsequently grow a full size crystal (100-200 gr.) of L- α -alanine doped DTGS and TGS respectively (LADTGS and LATGS). Initial efforts during the end of the third reporting period only permitted examining a relatively small seed crystal grown from triple deuterated TGS doped with L- α -alanine at 42-41°C. The Curie temperature was found to be 62.3°C. Initial values for pyroelectric coefficient, dielectric constant, loss tangent, and figures of merit at 40°C only are shown for LADTGS in Appendix A. At 40°C, without any bias, the lowest loss tangent was obtained which leads one to suspect that the lowest loss tangent (and the highest degree of self-bias) is obtained around the temperature at which the crystal was grown. All excursions in temperature above or below the crystal growth temperature cause additional stresses. To reach minimum loss tangent and dielectric constant at 40°C after a 20°C drop from 60°C

was found to take some 24 hours. The measured loss tangents on initially reaching 40°C were at least an order of magnitude higher compared to the values obtained after maintaining the sample for 24 hours at 40°C. Final values were as follows:

frequency	$\tan \delta \times 10^{-3}$ (40°C)
100 Hz	3
1K Hz	2.3
10K Hz	1.1
100K Hz	0.1

At this time the performance of LADTGS over the entire range from -30°C to 80°C is still being evaluated.

3.3 Detector Responsivity and Noise Measurement

The source-follower circuit (Figure 4-6, first quarterly report) employing the FET with the lowest leakage current (I_{GSS} , Table 4-1, and Figures 4-13, 4-14, 4-15, second quarterly report), namely Siliconix FN2182A, has been completed. All future detectors will be evaluated using this one FET to reduce the additional possibility of variation between FET's.

The post-amplifier (actually labeled pre-amplifier in Figure 4-7, first quarterly report) employing a Siliconix 2N4868A, having the lowest measured short circuit current noise (equivalent to the short circuit noise at post-amplifier shown in Figure 4-18, second quarterly report) has also been completed.

As soon as individual detector elements are completed, the above equipment in conjunction with a blackbody radiation source, chopper, and wave analyzer will be used to determine responsivity, noise, and detectivity as a function of frequency, and detector temperature.

Section 4.0 NEW TECHNOLOGY

During this report period there were no technical developments reportable under the New Technology Clause of the subject contract.

Section 5.0 PLANNED FOR NEXT REPORT PERIOD

To best utilize the reduced funding for fiscal 1973, the tasks outlined below, to be accomplished during a six months period, are recommended:

1. Grow 1 crystal of L- α -alanine doped TGS and 1 crystal of L- α -alanine doped DTGS.
2. For the materials in Item 1 measure the pyroelectric coefficient as a function of temperature from -30°C to approximately 80°C , and the dielectric constant plus loss tangent over the same temperature range as a function of frequency. Also complete the dielectric constant and loss tangent measurements on TGFB, EDT, and TGS 0.88-TGFB 0.12, whose pyroelectric coefficients have been previously measured.
3. Mount 1.5mm x 1.5mm x 0.03mm detector flakes fabricated from respectively L- α -alanine doped TGS, L- α -alanine doped DTGS, gamma irradiated TGS, gamma irradiated DTGS, gamma irradiated TGFB, LiTaO_3 , PLZT 4/60/40, $\text{Sr}_{0.75}\text{Ba}_{0.25} \cdot \text{Nb}_2\text{O}_6$, and PbTiO_3 ($\sim 0.1\text{UO}_3$ doped) and then measure responsivity and noise as a function of chopping frequency and temperature.
4. Complete low temperature measurements on FETs listed in the quarterly report. Completely test approximately 10 new FET types not previously tested.
5. Construct complete detectors, including low noise FETs, selected from the three materials showing promise of providing the highest detectivity.
6. Write one Quarterly and one Final Report.

Section 6.0 CONCLUSION AND RECOMMENDATIONS

The project accomplishments during the reporting period are consistent with the overall objectives of the program to develop pyroelectric detectors of improved detectivity. Since the project is being funded at a reduced rate, a system of priorities had to be established. The investigation of such materials as NaNO_2 , glucuronolactone, polyvinyl fluoride, and polyvinylidene fluoride for I.R. detectors had to be shelved. Future investigations should look into these materials.

Determination of pyroelectric material parameters (i.e. pyroelectric constant, dielectric constant, and loss tangent) as function of temperature and frequency are almost completed. The compilation of pyroelectric materials characteristics has been brought up-to-date.

Fully poled TGS, DTGS, and TGFB, after gamma irradiation with approximately 2 MegaRontgen from a Cobalt 60 source, exhibit "locked-in" polarization. A similar effect is obtained by doping with L- α -alanine.

The pyroelectric parameters of Li_2TaO_3 compare favorably with those of TGS and DTGS. Its high Curie temperature (1200°C) prevents depoling at all foreseeable operating temperatures. It will prove extremely useful wherever very high ambient temperatures or very high energy levels (as from a laser) are encountered. High responsivity and detectivity will prove to be rather constant over a wide temperature range. For optimum responsivity below 6μ it will need additional blackening.

Of the many currently available PLZT formulations, only the 4/60/40 composition (La:Zr:Ti) has been investigated under this program. Other compositions may turn out to have improved responsivity and detectivity figures of merit. Both PLZT and PZT pyroelectric materials are useful as laser energy detectors.

The $\text{Sr}_{0.75}\text{Ba}_{0.25}\text{Nb}_2\text{O}_6$ formulation does not appear as promising for an improved pyroelectric detector as was initially expected.

If a domestic supplier of doped PbTiO_3 crystal cannot be found, it is recommended that future work concern itself with growing and analyzing this material further as a pyroelectric detector material.

APPENDIX A - COMPILATION OF PYROELECTRIC MATERIALS AND THEIR
CHARACTERISTICS AS DERIVED FROM A SURVEY OF THE LITERATURE.

TABLE A-1. PYROELECTRIC MATERIALS CHARACTERISTICS

MATERIAL	Curie Temperature T _c °C	Temperature of Measurement	Dielectric Constant ε at 1kHz*	Spontaneous Polarization P _s C cm ⁻² x 10 ⁻⁶	Pyroelectric Constant dP _s /dT C cm ⁻² K ⁻¹ x 10 ⁻⁸	Specific Heat c J cm ⁻³ K ⁻¹	Density ρ	A.C. Resistivity (1 KHz) ρ	(dP _s /dT) ε ⁻¹ x 10 ⁻¹⁰	(dP _s /dT) ε ⁻¹ x 10 ⁻¹⁰	(dP _s /dT) ε ^{-1/2} x 10 ⁻⁴	Reference	COMMENTS
LiNbO ₃	1200	27 100 200 450	30 30 (100kHz) 30 (100kHz) 40 (100kHz)	50 49.5 49 46	0.4 0.5 0.7	2.8	4.65	9.8 x 10 ¹⁰	1.3 1.7 2.3	0.46 0.61 0.82	4.5	N1, P1, S1	T _c depends on crystal composition; varies from 1150° - 1240° C. Transmits 0.4-5μ.
LiTaO ₃ (Crystal Technology)	660, 618 for Ta/Li = 1.1	0 25 50 250 (10kHz) 450 (10kHz)	<u>52</u> 54 <u>56</u> 70 (10kHz) 300 (10kHz)	50 50 45 37.7	<u>2.2</u> <u>2.3</u> <u>2.3</u> 2.1 8.2	3.16 3.72 3.84	7.45	<u>4.4 x 10¹⁰</u> <u>3.6 x 10¹⁰</u> <u>2.9 x 10¹⁰</u>	<u>4.1</u> 4.3 <u>4.5</u> 3.0 2.7	1.3 1.3 1.4 0.81 0.71	14.6 13.8 13.4	G1, G2 M1, Y1 I1, G6	T _c depends on crystal composition, varies from 560° - 660° C. Transmits 0.5 to 6 microns
PbTiO ₃ (~0.1 UO ₃)	492	25	200	60	6	3.23	7.78	1 x 10 ⁹	3	0.93	6	B7, B3, R2, S11, S12, S13, Y4	Transmits 0.6 to 6μ. T _c depends on crystal composition Constant responsivity -20° to 50° C.
PZT 5A (Clevite)	365	25	1900	38	4.0	3.1	7.75	4.7 x 10 ⁷	0.21	0.068	0.89	L1, C1	
PZT 4 (Clevite)	328	25	1400	30	3.7	3.0	7.5	3.2 x 10 ⁸	0.26	0.087	2.2	L1, C1	
PZT G-1306 (Gulton)	290	0 25 50	<u>1560</u> 1720 <u>1900</u>		<u>4.3</u> <u>4.3</u> <u>4.3</u>	0.0	(7.6)	<u>5.9 x 10⁷</u> <u>3.7 x 10⁷</u> <u>5.4 x 10⁷</u>	<u>0.28</u> <u>0.43</u> <u>0.23</u>	<u>0.092</u> <u>0.082</u> <u>0.073</u>	1.1 1.1 1.1		
PZT HST-41 (Gulton)	270	25	1800	23	2	3.0	7.6	4.5 x 10 ⁷	0.11	0.037	0.45	L2, G8	Transmits 0.4 to ~9μ.
5 Pb 0.3CeO ₂	177	50	60 (10kHz)	4.5	1				1.7			I2	
PZT 4/60/40 (Honeywell)	218	0 25 50	740 850 <u>1020</u>		<u>4.9</u> <u>5.6</u> <u>6.3</u>	2.6	7.85	<u>4.9 x 10⁷</u> <u>3.0 x 10⁷</u> <u>2.0 x 10⁷</u>	<u>0.66</u> <u>0.65</u> <u>0.62</u>	0.25 0.25 0.24	1.3 1.2 1.1		
PLTZ 6.5/65/35 (Honeywell)	164	27	1400		10	2.6	7.83	5.1 x 10 ⁷	0.71	0.23	2.8	H6, H8, L4	
Ge ₂ (MoO ₄) ₃	161	25 100 143	10 10 10	0.2 0.15 0.1	0.1 0.14	2.1 2.1	4.6		1.0 1.4	0.48 0.67		K1, R1 U1, U2 C2, P1, K7	Does not exhibit dielectric anomaly at Curie temp. Operates as a laser with Nd ³⁺ doping. Ferroelastic. Transmits 0.3-9microns
NaNO ₂	160	25	8	7	0.4	2.0	2.1	>10 ¹¹	5	2.5	>6.3	S2, P1	ε practically constant to 140° C.

Values in parentheses are based on assumptions. Underlined values represent measurements at BEC. *Units: otherwise noted. REV. B

TABLE A-1. PYROELECTRIC MATERIALS CHARACTERISTICS (CONTINUED)

MATERIAL	Curie Temperature T _c °C	Temperature of Measurement t °C	Dielectric Constant ε at 1kHz*	Polarization P _s C cm ⁻² x 10 ⁻⁶	Pyroelectric Constant dP _s /dT C cm ⁻² °K ⁻¹ x 10 ⁻⁸	Specific Heat c J cm ⁻³ °K ⁻¹	Density s g cm ⁻³	A.C. Resistivity (1 KHz) ρ Ω-cm	(dP _s /dT) ε ⁻¹ x 10 ⁻¹⁰	(dP _s /dT) (ε ⁻¹) x 10 ⁻¹⁰	(dP _s /dT) ρ ^{1/2} ε ⁻¹ x 10 ⁻⁴	Reference	COMMENTS
BaTiO ₃ (single crystal)	120	23 60 100	200	26 24 20	5 7 20	3.0	6.0	6x10 ⁶	3.5	1.2	0.57	P1, H1 C3, H1, P1	Absorbs 0.7 to 2μ (I3) Cannot be fully poled (S3)
SBN, x=0.52 (A)	115	25	380	29.2	6.5	2.1	5.2	1.6x10 ⁸	1.7	0.81	4.0	B1, G3, G4	Transmits 0.5-6 microns (B4)
SBN, x=0.33	62	25	1800	23.3	11			1.2x10 ⁸	0.61	0.29	5.8		
SBN, x=0.25 (crystal technology)	30	0	2500**	18	12			5.1x10 ^{7**}	0.48	0.23	4.1		
		25	5000**		37			1.9x10 ^{7**}	0.74	0.32	7.7		
		50	12000**		10			6.5x10 ^{6**}	0.083	0.04	1.2		
NH ₄ IO ₃	85	26	30	0.7	0.3		3.3	2.9x10 ⁸	1.0			C4, K4	Transmits 0.35 - 2 microns Explodes above 180°C
TGFB(B)	74.7	0			1.2								
		25	11 (10kHz)	3.7	2.1	2.6	1.66	19.1	7.3			R3, H2, S4, W1	Transmits 0.24 - 2 microns
		50	20 (10kHz)	3.1	4.6	3.1		23.0	7.4				
TGFB + 2.3Mr (Co60)	72	0	10		1.2	(2.4)	1.66	1.0x10 ¹¹	12.0	5.0	15.8		No depoling below T _c
		25	14		2.1	(2.6)		5.8x10 ¹⁰	15.0	5.8	19.4		
		50	30		5.6	(3.1)		2.0x10 ¹⁰	18.7	6.0	25.5		
DTGS(C)	61	0	12**		0.8	(2.4)	(1.7)	5.0x10 ^{10**}	6.7	2.8	7.5	B3, S5	T _c depends on D ₂ substitution for H ₂ up to a maximum possible of 64.8%. Transmits 0.24-2.3 microns No depoling below T _c
		25	18**	2.6	2.7	(2.5)		5.0x10 ^{10**}	15.0	6.0	24.2		
		50	60**	1.8	10.0	(2.8)		1.2x10 ^{10**}	16.7	6.0	39.3		
DTGS + 2.3Mr (Co 60)	59.5	0	11.5		0.52	(2.4)	(1.7)	4.7x10 ¹⁰	4.5	1.9	4.7		
		25	20		3.0	(2.5)		4.1x10 ¹⁰	15.0	6.0	24.4		
		50	110		12.0	(2.8)		2.3x10 ⁹	10.9	3.9	20.6		
DTGS+L-α-alanine***	62.3	40	33.2		4.6	(2.7)	(1.7)	2.4x10 ¹⁰	13.8	5.1	26.4	K5, K6, J5	No depoling below T _c
TGS _{0.67} TGFB _{0.33}	58.9	25		2.9	3.0							B5	TGS:TGFB ratio can be varied to vary T _c
		50		1.75	8.2								
TGS _{0.88} TGFB _{0.12}	55.5	0			1.9								
		25			4.0								
		50			20.0								
KTN (D) x=0.57	54	25	900*** (800Hz)	9.3	1.7	(2.3)		2.4x10 ¹⁰	0.2	2.8	8.8	A1	Transmits out to 6 microns. KTaO ₃ and KNbO ₃ form solid solution. Parameters depend on composition (C6, J1)
		40	1600*** (600Hz)	8.4	13			2.4x10 ¹⁰	0.8	2.8	12.9		
		0	20**		1.3			8.7	6.5	4.6	17.1		
		10	23**	3.0	2.0	2.4	1.66	2.4x10 ¹⁰	6.5	2.8	8.8		Absorbs below 0.24 microns (S9), and between 2 to 400 microns (M2). Transmits 0.25 - 2 microns. Doping, x-ray, u.v. irradiation effect parameters (C8, H3, S9, Y2, Y3, W6, Z1). Loss tangent increases below ambient temp (I-4).
		25	35**	2.75	4.0	2.5		1.7x10 ¹⁰	11.4	4.6	20.9		
		40	100**	2.0	12.0	2.8		1.6x10 ⁹	12.0	4.3	17.1		

Values in parentheses are based on assumptions. Underlined values represent measurements at BEC. *Unless otherwise noted **5kV/cm bias ***preliminary data ****kV/cm bias REV. B

TABLE A-1. PYROELECTRIC MATERIALS CHARACTERISTICS (CONTINUED)

MATERIAL	Curie Temperature T_c °C	Temperature of Measurement T °C	Dielectric Constant ϵ at 1kHz *	Spontaneous Polarization P_s C cm ⁻² $\times 10^{-6}$	Pyroelectric Constant dP_s/dT C cm ⁻² °K ⁻¹ $\times 10^{-6}$	Specific Heat c J cm ⁻³ °K ⁻¹	Density ρ g cm ⁻³	A.C. Relativity (1 KHz)	$(dP_s/dT) \epsilon^{-1}$ $\times 10^{-10}$	$(dP_s/dT) \epsilon^{-1}$ $\times 10^{-10}$	$(dP_s/dT) \rho^{1/2} \epsilon^{-1}$ $\times 10^{-4}$	Reference	COMMENTS
TGS/Se (~15%Se) +L-α-alanine	49	25	28 (10kHz)		5	2.5	(1.66)	4×10^9	17.8	7.1	12.7	P2	Mullard (U.K.) Development; Material does not depole $T < T_c$.
TGS/Se (~5%Se) 'after treatment'	47	25	26 (10kHz)		4.1	2.5	(1.66)	5×10^9	15.8	6.3	11.7	P2	Mullard (U.K.) Development; Material does not depole $T < T_c$.
DTGS (F)	34.5	25	(~100)	3.2	7.5	(2.3)	(1.9)		7.5	3.3		M3	No depoling below T_c
TGS+2.3Mr (Co 60)	47.4	0 25 40	16.5 40.0 150.0		2.2 5.0 13.0	(2.3) (2.5) (2.8)	1.66	8.4×10^{10} 2.8×10^{10} 2.4×10^9	13.3 12.5 8.7	5.8 5.0 3.1	27.7 33.5 22.8		
TGS (G)	23.4	0 15	(~100)	3.0 2.6	13	2.1 2.3	(1.9)		13	5.7		D4, G7; H2, M3, R3, S7, S8,	
Li ₂ SO ₄ · H ₂ O	(M)	25 50	12.2 12.3	0.8 1	1.16 1.60	2.3	2.06	1×10^{11} 7×10^{10}	9.5 13.0	4.1 5.6	15.9 18.4	L1, A2, L3, W2	Withstands up to 95% R.H. (C1). Flat response over a wide temperature range (B1, M3). Transmits 0.2-2.4 microns; 3.2-4.2 microns
Li ₂ SeO ₄ · H ₂ O		20 79			0.57 0.65		(2.8)					A2	
Polyvinylidene fluoride (CH ₂ CF ₂) _n	not known, softens at 150°C melts at 177°C	25	11	2	0.24	2.4		6.5×10^9	2.2	0.9	0.81	B2, G5	Transmits 0.4-2μ, absorbs 3-300μ; T_c (if it exists) may be near the melting point (N2)

Values in parentheses are based on assumptions. Underlined values represent measurements at BEC. *Unless otherwise noted **skv/cm bias ***preliminary data ****kv/cm bias REV B

TABLE A-1. PYROELECTRIC MATERIALS CHARACTERISTICS (CONTINUED)

MATERIAL	Curie Temperature T_c °C	Temperature of Measurement T °C	Dielectric Constant ϵ at 1kHz *	Spontaneous Polarization P_s $C \text{ cm}^{-2} \times 10^{-6}$	Pyroelectric Constant dP_s/dT $C \text{ cm}^{-2} \text{ } ^\circ K^{-1} \times 10^{-6}$	Specific Heat c $J \text{ cm}^{-3} \text{ } ^\circ K^{-1}$	Density ρ $g \text{ cm}^{-3}$	A.C. Resistivity (1 KHz) ρ $\Omega \text{ - cm}$	$(dP_s/dT) \epsilon^{-1}$ $\times 10^{-10}$	$(dP_s/dT) \epsilon^{-1}$ $\times 10^{-10}$	$(dP_s/dT) \rho^{1/2} \epsilon^{-1}$ $\times 10^{-4}$	Reference	COMMENTS
SbSI	22	0	2200	22								F2	Also photoconductive (U3)
		10	2500	15	60	2.38	8.2		2.4	1.0		W2	
		15	3000	12	100				3.3	1.4			
GASH ^(H)	(M)	25	6	0.35	0.15	~ 1			2.5	2.5	4.5	H4, P1, N3	Ge isomorph (for Al), SeO ₄ isomorph (for SO ₄), (Ge and SeO ₄) isomorph (for Al and SO ₄). Similar performance (H4)
GUL (I)		25	4.6		0.62	~ 1.5			13.5	9	26	P1	
EDT (I)		25	7.0		0.2	~ 1			3	3	>6	P1	dP_s/dT is constant from 20° to 80°C (N3) transmits 0.24 - 2 microns
Colemanite (K)	-7	-10 -20	60 12	0.29 0.46	5.4 1.2	0.58	2.42		9 10	15.5 17		W3, C7	Depending on purity, T_c of 2.5°C is also reported (D2). Synthetic strontium isomorphs (polycrystalline) have been grown (W4, W5).
KDDP (L)	-50±2	-60	50	4.0	10		2.36	8.6×10^7	20			M4, A3	Transmits 0.2 to 2μ.
(NH ₂ CH ₂ COOH)·HNO ₃	-67	-77	50 (10kHz)	0.6	5	2.0	1.58		10	5		P3	
		-190	15 (10kHz)	1.5	0.13				0.87				
CS(NH ₂) ₂ (Thiourea)	-104	-178	400	3.4	1		1.40		0.25			G9	
KH ₂ PO ₄ (KDP)	-150	-178	2500	4.8	3.3	0.94	2.34	7.2×10^6	0.13	0.14	1	B7, A3, D3, K3, S10	Transmits 0.2 to 2μ.

Values in parentheses are based on assumptions. Underlined values represent measurements at 8°C. *Unless otherwise noted **5kv/cm bias ***preliminary data ****4kv/cm bias

REV. B

TABLE A-1. PYROELECTRIC MATERIALS CHARACTERISTICS (CONTINUED)

NOTES

A	SBN = $\text{Sr}_{1-x}\text{Ba}_x\text{Nb}_2\text{O}_6$
B	TGFB = $(\text{NH}_2\text{CH}_2\text{COOH})_3\text{H}_2\text{BeF}_4$
C	DTGS = $(\text{ND}_2\text{CH}_2\text{COOD})_3\text{D}_2\text{SO}_4$
D	KTN = $\text{KTa}_{0.57}\text{Nb}_{0.43}\text{O}_3$
E	TGS = $(\text{NH}_2\text{CH}_2\text{COOH})_3\text{H}_2\text{SO}_4$
F	DTGSe = $(\text{ND}_2\text{CH}_2\text{COOH})_3\text{D}_2\text{SeO}_4$
G	TGSe = $(\text{NH}_2\text{CH}_2\text{COOH})_3\text{H}_2\text{SeO}_4$
H	GASH = $(\text{CN}_3\text{H}_6\text{Al}(\text{SO}_4)_2 \cdot 6\text{H}_2\text{O})$
I	GUL = Glucuronolactone = $\text{CO} \cdot (\text{CHOH})_2 \cdot \text{CH}(\text{O}) \cdot \text{CHOH} \cdot \text{CHO}$
J	EDT = $\text{C}_2\text{H}_4(\text{NH}_3)_2\text{C}_4\text{H}_4\text{O}_6$
K	Colemanite = $2\text{CaO} \cdot 3\text{B}_2\text{O}_3 \cdot 5\text{H}_2\text{O}$
L	KDDP = KD_2PO_4 (~90% D_2)
M	Decomposes before T_c can be measured.

REFERENCES

- (A 1) ANISTRATOV, A. T., Trans, 6th Int. Conf. Ferroelectricity, Riga, 1014 (May 1968).
- (A 2) ACKERMANN, W., Ann. Physik, 46, 197 (1915).
- (A 3) AZOULAY, J., GRINBERG, Y., PELAH, I., WIENER, E., J. Phys. Chem. Solids, 29, 843 (1968).
- (B 1) BEERMAN, H. P., Ferroelectrics, 2, 123 (1971).
- (B 2) BERGMAN, J. G., McFEE, J. H., CRANE, G. R., Appl. Phys. Letters, 18, 203 (1971).
- (B 3) BREZINA, B., STMUTNÝ, B., Czech. J. Phys., B 18, 393 (1968).
- (B 4) BRICE, J. C., HILL, O. F., WHIFFIN, P. A. C., WILKINSON, J. A., J. Crystal Growth, 10, 133 (1971).
- (B 5) BREZINA, B., ŠAFRÁNKOVÁ, M., KVAPIL, J., Phys. Stat. Sol., 15, 451 (1966).
- (B 6) BUSCH, G., Helv. Phys. Acta, 11, 269 (1938).
- (B 7) BHIDE, V. G., HEDGE, M. S., DESHMUKH, K. G., J. Am. Ceramic Soc., 51, 565, (1968).
- (B 8) BHIDE, V. G., DESHMUKH, K. G., HEDGE, M. S., Physics, 28, 871, (1962).
- (C 1) Clevite Corp. Data (1965).
- (C 2) CUMMINS, S. E., Ferroelectrics, 1, 11 (1970).
- (C 3) CHYNOWETH, A. G., J. Appl. Phys., 27, 78 (1956).
- (C 4) CRANE, G. R., BERGMAN, J. G., GLASS, A. M., J. Am. Ceramic Soc., 52, 655, (1969)
- (C 5) CHYNOWETH, A. G., Phys. Rev., 117, 1235 (1960).
- (C 6) CHEN, F. S., GEUSIC, J. E., KURTZ, S. K., SKINNER, J. G., WEMPLE, S. H., J. Appl. Phys., 37, 388 (1966).
- (C 7) CHYNOWETH, A. G., Acta Crys., 10, 511 (1957).
- (C 8) CHYNOWETH, A. G., U. S. Pat. 3,005,096, Oct. 17, 1961.

- (D 1) DIMAROVA, E. N., POPLAVKO, Yu. M., Trans. 6th Int. Conf. Ferroelectricity, Riga, 332 (May 1968).
- (D 2) DAVISSON, J. W., Acta Cryst., 9, 9 (1956).
- (D 3) DeQUERVAIN, M., Helv. Phys. Acta, 17, 509 (1944).
- (D 4) DUDEK, J., Acta Phys. Pol. A39, 675, (1971).
- (F 1) FOUSKOVA, A., J. Phys. Soc. Japan, 27, 1699 (1969).
- (F 2) FATUZZO, E., HARBECKE, G., MERZ, W. J., NITSCHKE, R., ROETSCHI, H., RUPPEL, W., Phys. Rev., 127, 2036 (1962).
- (F 3) FURUKAWA T., VEMATSU, Y., ASAKAWA, K., WADA, Y., J. Appl. Polymer Sci., 12, 2675, (1968).
- (G 1) GLASS, A. M., Phys. Rev., 172, 564 (1968).
- (G 2) GLASS, A. M., ABRAMS, R. L., J. Appl. Phys., 41, 4455 (1970).
- (G 3) GLASS, A. M., J. Appl. Phys., 40, 4699 (1969).
- (G 4) GLASS, A. M., Appl. Phys. Letters, 13, 147 (1968).
- (G 5) GLASS, A. M., McFEE, J. H., BERGMAN, J. G., J. Appl. Physics, 42, 5219, (1971)
- (G 6) GLASS, A. M., Private Communication of Value ρ .
- (G 7) GAVRILOVA, N. D., NOVIK, V. K., KOPTSIK, V. A., Sov. Phys.-Cryst., 13, 949 (1969).
- (G 8) GULTON INDUSTRIES, INC., (Metuchen, N. J.) - Glennite Piezoceramics Data.
- (G 9) GOLDSMITH, G. J., WHITE, J. G., J. Chem. Phys., 31, 1175 (1959).
- (H 1) HADNI, A., Optics Comm., 1, 251 (1969).
- (H 2) HOSHINO, S., MITSUI, T., JONA, F., PEPINSKY, R., Phys. Rev., 107, 1255 (1957).
- (H 3) HILCZER, B., Trans. 6th Int. Conf. Ferroelectricity, (Riga 1968), 1023.
- (H 4) HOLDEN, A. N., MERZ, W. J., REMEIKA, J. P., MATHIAS, B. T., Phys. Rev., 101, 962 (1956).

- (H 5) HEILAND, G., IBACH, H., Solid State Comm., 4, 353, (1966).
- (H 6) HAERTLING, G. H., LAND, C. E., J. Am. Ceramic Soc., 54, 1, (1971).
- (H 7) HOSHINO, S., OKAYA, Y., PEPINSKY, R., Physics Rev., 115, 323 (1959).
- (H 8) HAERTLING, G. H., LAND, C. E., Ferroelectrics, 3, 269, (1972) or IEEE, Trans, Sonics & Ultrasonics, SU-19, 269 (1972).
- (I 1) IWASAKI, H., UCHIDA, N., YAMADA, T., Japan J. Appl. Phys., 6, 1336 (1967).
- (I 2) IWASAKI, H., SUGII, K., YAMADA, T., NIIZEKI, N., Appl. Phys. Letters, 18, 444 (1971).
- (I 3) IWASAKI, H., J. Radio Research Lab., Japan, 17, 147 (1970).
- (I 4) ITOH, K., MITSUI, T., J. Phys. Soc. Japan, 23, 334 (1967).
- (K 1) KUMATA, A., YUMOTO, H., ASHIDA, S., J. Phys. Soc. Japan, 28, 351 (1970 Supplement).
- (K 2) KREMENCHUGSKII, L. S., SAMOILOV, V. B., Sov. Phys.-Cryst., 12, 940 (1968).
- (K 3) KAMYSHEVA, L. N., et al., Acad. Sci., USSR, Bull. Phys. Ser. 31, 1202 (1967).
- (K 4) KEVE, E. T., ABRAHAMS, S. C., BERNSTEIN, J. L., J. Chem. Phys., 54, 2556, (1971).
- (K 5) KEVE, E. T., BYE, K. L., WHIPPS, P. W., ANNIS, A. D., Journal du Physique - to be published.
- (K 6) KEVE, E. T., BYE, K. L., WHIPPS, P. N., ANNIS, A. D., Ferroelectricity, 3, 39, (1971).
- (K 7) KUMADA, A., Ferroelectrics, 3, 115, (1972) or IEEE Trans. Sonics & Ultrasonics, SU-19, 115, (1972).
- (L 1) LANG, S. B., NBS Report No. 9289, (7-28-1967).
- (L 2) LACHAMBRE, J. L., Rev. Sci. Inst., 42, 74 (1971).
- (L 3) LANG, S., Phys. Rev. B., 4, 3603, (1971).

- (L 4) LIU, S. T., HEAPS, J. D., TUFTE, O. N., *Ferroelectrics*, 3, 281 (1972), or *IEEE Trans. Sonics and Ultrasonics*, SU-19, 281, (1972).
- (L 5) LOCK, P. J., *Appl. Phys. Letters*, 19, 390, (1971).
- (M 1) MATTHIAS, B. T., *Science* 113, 591 (1951).
- (M 2) MÖLLER, K., FAIRLEIGH DICKINSON U., private communication.
- (M 3) MÁLEK, Z., ŠTRAJBLOVÁ, J., NOVOTNÝ, J., MAREČEK, V., *Czech. J. Phys. B* 18, 1226 (1968).
- (M 4) MILEK, J. T., WELLES, S. J., Linear Electrooptics Modulator Materials, Air Force Materials Lab, Air Force Systems Command Contract F33615-68C-1225 to Hughes Aircraft Co., S-14, 143 (Jan. 1970).
- (M 5) McFEE, J. H., BERGMAN, J. G., CRANE, G. R., *Ferroelectrics*, 3, 305, (1972) and *IEEE Trans. Sonics & Ultrasonics*, SU-19, 305, (1972).
- (N 1) NASSAU, K., LEVINSTEIN, H. J., LOIACONO, G. M., *J. Phys. Chem. Solids*, 27, 989 (1966).
- (N 2) NAKAMURA, K., WADA, Y., *J. Polymer Sc.; Part A-2*, 9, 161 (1971).
- (N 3) NOVIK, V. K., *Sov. Phys.-Cryst.*, 10, 89 (1965).
- (P 1) PUTLEY, E. H., *Proc. Symp. Submillimeter Waves*, (N. Y. 1970), 267.
- (P 2) PUTLEY, E. H., "Pyroelectric Detectors and Their Application in Thermal Imaging Systems," R. R. E. Malvern, Worcs, U. K. - to be published.
- (P 3) PEPINSKY, R., VEDAM, K., HOSHINO, S., OKAYA, Y., *Phys. Rev.* 111, 430 (1958).
- (P 4) PHELAN, R. J., MAHLER, R. J., COOK, A. R., *Appl. Phys. Letters*, 19, 337, (1971).
- (R 1) RABINOVICH, A. Z., ROITBERG, M. B., *Sov. Phys.-Cryst.*, 15, 1023 (May-June 1971).
- (R 2) REMEIKA, J. P., GLASS, A. M., *Met. Res. Bul.*, 5, 37 (1970).
- (R 3) REMOISSENET, M., GODEFROY, L., *C. R. Acad. Sc. Paris*, 266, 948 (1968).

- (S 1) SAVAGE, A., J. Appl. Phys., 37, 3071 (1966).
- (S 2) SAWADA, S., NOMURA, S., FUJII, S., YOSHIDA, I., Phys. Rev. Letters, 1, 320 (1958).
- (S 3) SANDERS ASSOC. - private communications.
- (S 4) STRUKOV, B. A., Proc. Int. Meeting Ferroelectricity, Prague, 1, 191 (1966).
- (S 5) SIL'VESTROVA, I. M., Sov. Phys. - Cryst., 6, 466 (1962).
- (S 6) STRUKOV, B. A., Sov. Phys. - Solid State, 6, 2278 (1965).
- (S 7) STRUKOV, B. A., TARASKIN, S. A., KOPTSIK, V. A., VARIKASH, V. M., Sov. Phys. - Cryst., 13, 447 (1968).
- (S 8) STRUKOV, B. A., TARASKIN, S. A., VARIKASH, V. M., Sov. Phys. - Solid State, 10, 1445 (1968).
- (S 9) SIL'VESTROVA, I. M., ROMANYUK, N. A., Sov. Phys. - Cryst., 5, 138 (1960).
- (S 10) STEPHENSON, C. C., HOOLEY, J. G., J. Am. Chem. Soc., 66, 1397 (1944).
- (S 11) SINGH, S., REMEIKA, J. P., POTOPOWICZ, J. R., Appl. Phys. Letters, 20, 135 (1972).
- (S 12) SHIRANE, G., HOSHINO, S., SUZUKI, K., Phys. Rev. 80, 1105, (1950).
- (S 13) SMOLENSKII, G. A., DOKLADY, A. K., Nauk SSSR, 70, 405, (1950).
- (T 1) TRIEBWASSER, S., Phys. Rev., 114, 63 (1959).
- (U 1) ULLMAN, F. G., GANGULY, B. N., ZEIDLER, J. R., Conf. Electronics Materials Comm. of AIME, S. Francisco (August 29 - Sept. 1, 1971). To be published J. Electronics Mat.
- (U 2) ULLMAN, F. G., GANGULY, B. N., HARDY, J. R., Ferroelectrics, 2, (1971) in press.
- (U 3) UEDA, S., TATSUZAKI, I., SHINDO, Y., Phys. Rev. Letters, 18, 453 (1967).

- (W 1) WIEDER, H. H., PARKERSON, C. R., J. Phys. Chem. Solids, 27, 247 (1966).
- (W 2) WILLARDSON, R. K., BEER, A. C., Ed., Semiconductors and Semimetals, 5, Academic Press, (N. Y. & London 1970), 260.
- (W 3) WIEDER, H. H., J. Appl. Phys., 30, 1010 (1959).
- (W 4) WIEDER, H. H., CLAWSON, A. R., PARKERSON, C. R., J. Appl. Phys., 33, 1720 (1962).
- (W 5) WIEDER, H. H., CLAWSON, A. R., PARKERSON, C. R., U.S. Patent No. 3,337,293.
- (W 6) WIEDER, H. H., PARKERSON, C. R., J. Phys. Chem. Solids, 25, 241 (1964).
- (Y 1) YAMADA, T., NIIZEKI, N., TOYODA, H., Japan, J. Appl. Phys., 7, 298 (1968).
- (Y 2) YURIN, V. A., SILVESTROVA, I. M., ZHELUDEV, I. S., Sov. Phys.-Cryst., 7, 312 (1962).
- (Y 3) YURIN, V. A., ZHELUDEV, I. S., Bull. Ac. Science USSR, 28, 633 (1964).
- (Y 4) YAMAKA, E., HAYASHI, T., MATSUMOTO, M., Infrared Phys., 11, 247 (1971).
- (Z 1) ZHELUDEV, I. S., Zh. Ludupov Ts., Ak. Nauk SSSR, Bull. Phys. Ser., 31, 1207 (1967).

APPENDIX B - MEASURED DATA ON SELECTED PYROELECTRIC MATERIALS -
OPTICAL TRANSMISSION - OPTICAL REFLECTANCE

EDP

0.1 mm

Beckman DK-2 CHART

WHEN REORDERING SPECIFY CHART NO. 566402 BECKMAN INSTRUMENTS INC. FULLERTON CALIF. U.S.A.

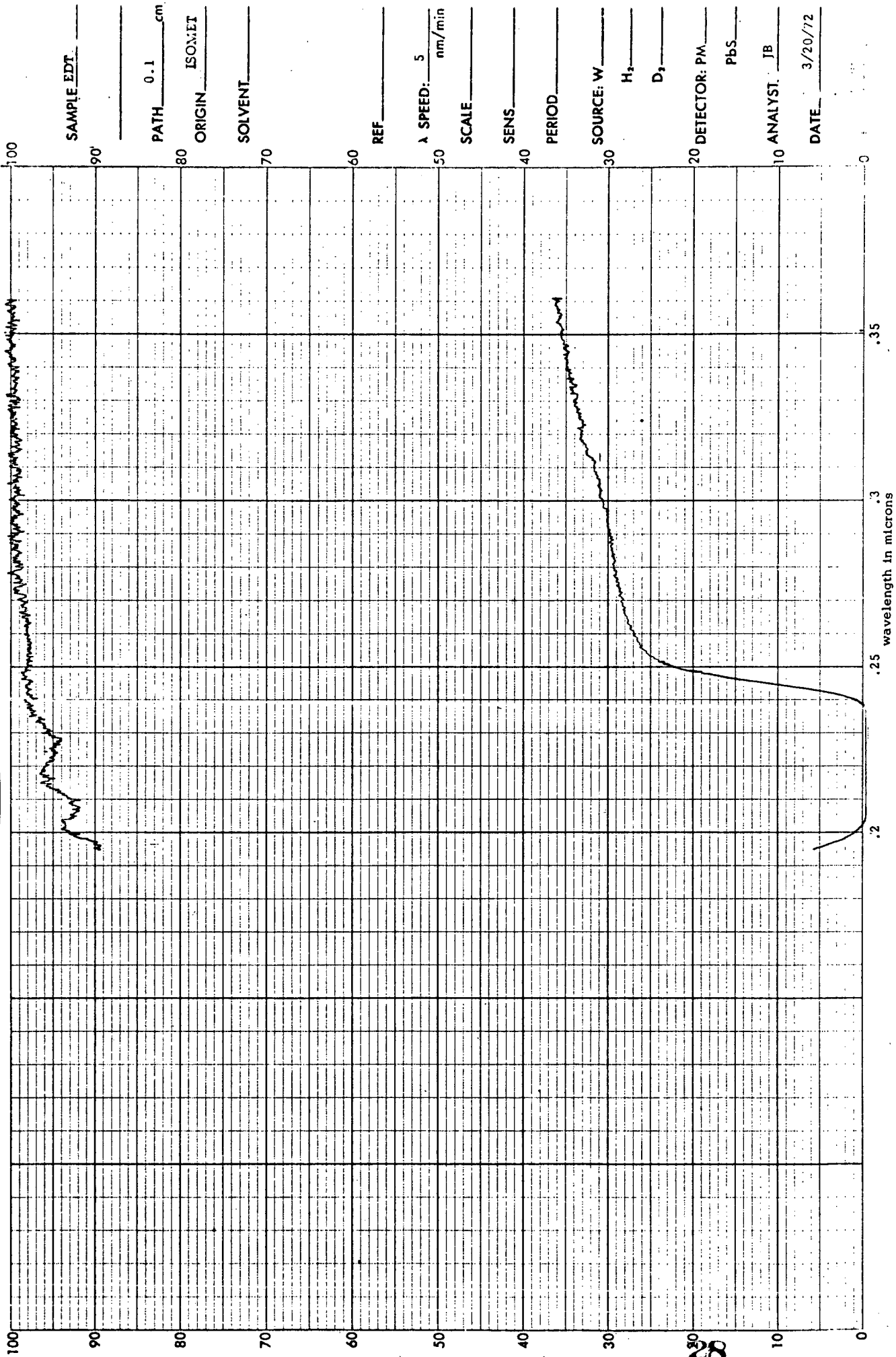
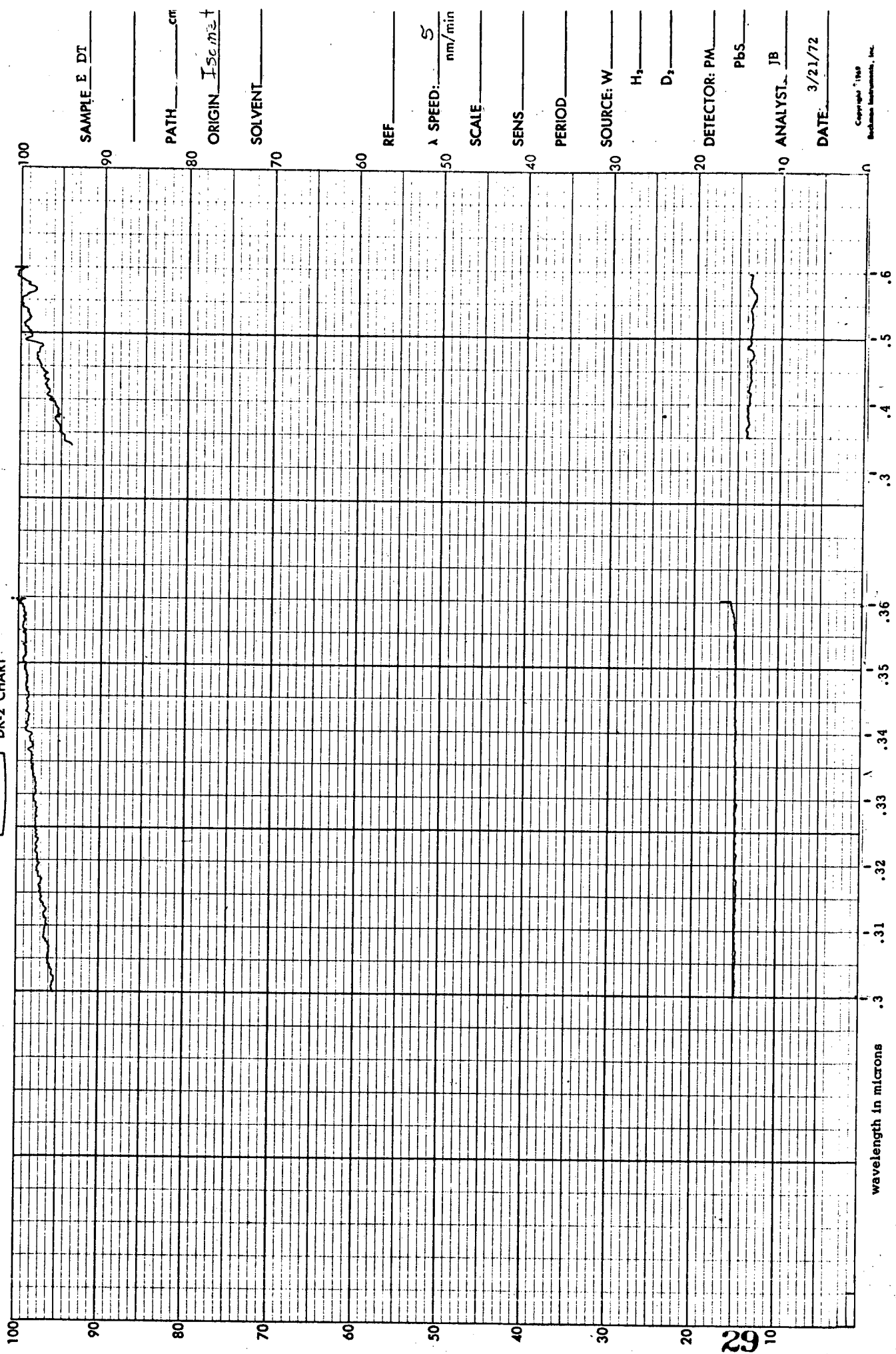


Figure B1.

Beckman DK-2 CHART

WHEN REORDERING SPECIFY CHART NO. 566402 BECKMAN INSTRUMENTS INC., FULLERTON, CALIF. U.S.A.



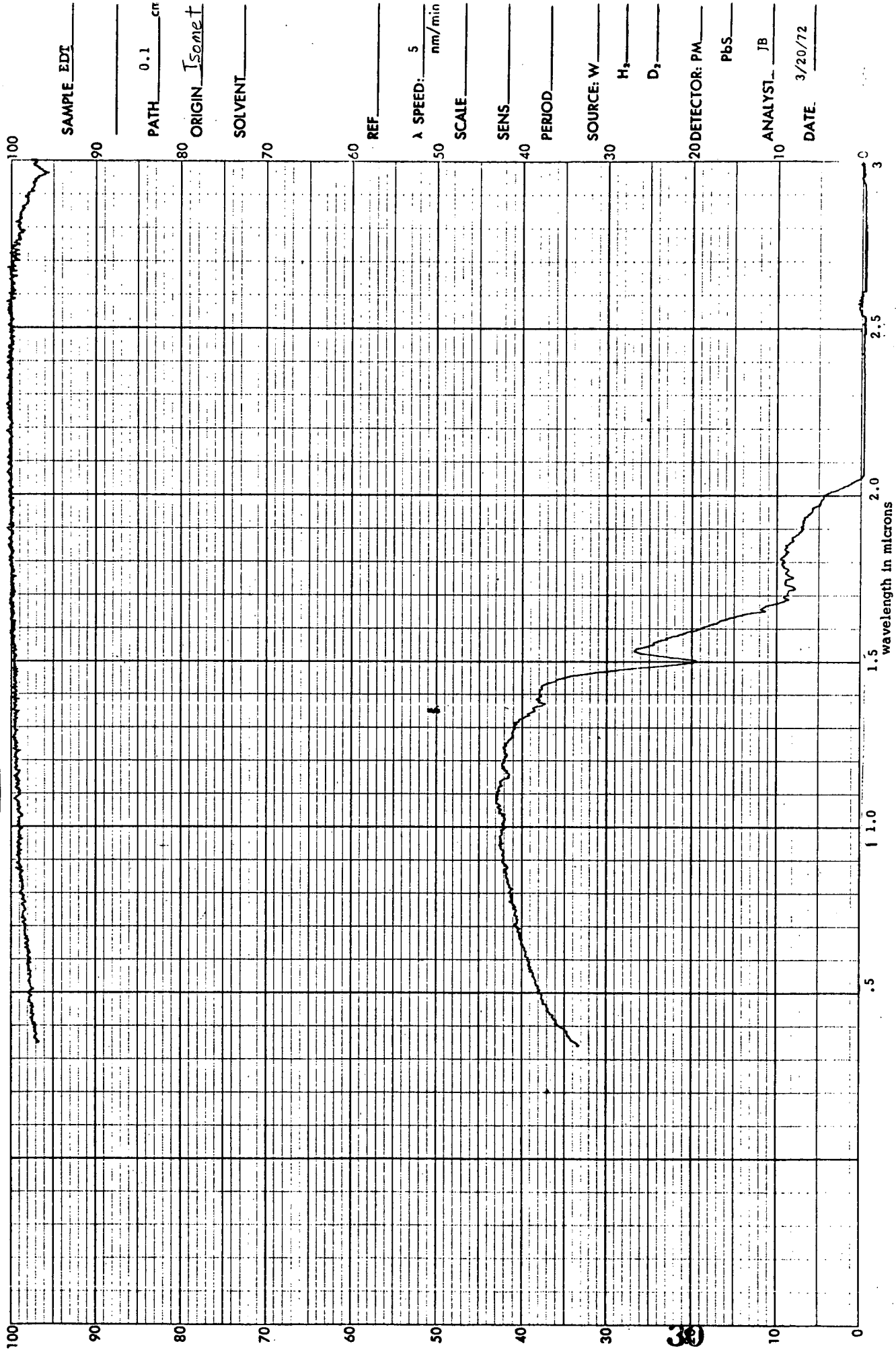
SAMPLE E DT _____
 PATH _____ cm
 ORIGIN Isomet
 SOLVENT _____
 REF _____
 λ SPEED: 5 nm/min
 SCALE _____
 SENS _____
 PERIOD _____
 SOURCE: W _____
 H₂ _____
 D₂ _____
 DETECTOR: PM _____
 PbS _____
 ANALYST: JB
 DATE: 3/21/72

Figure B2.

Beckman DK-2 CHART

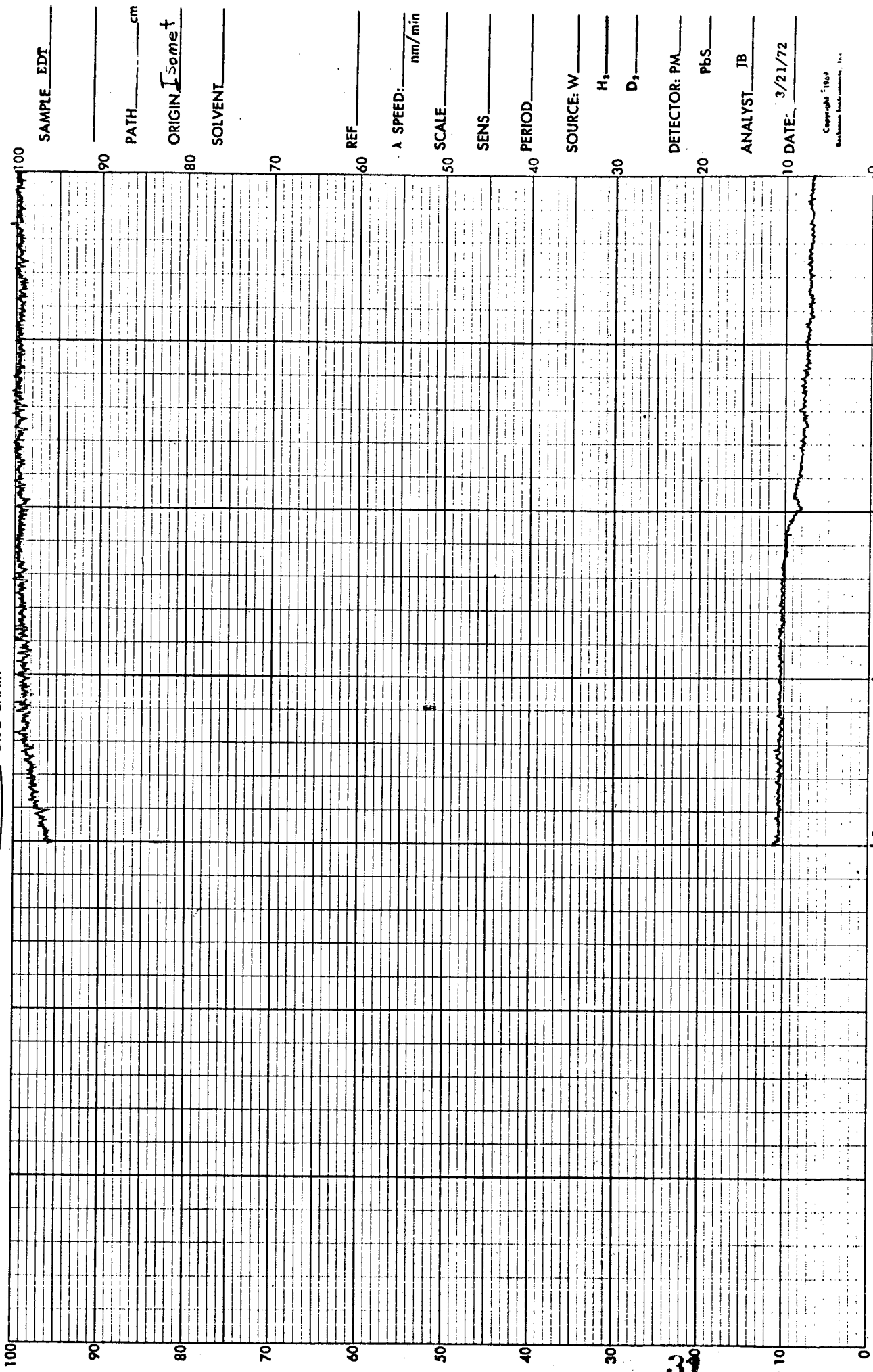
910

Printed in U.S.A. 97171740



SAMPLE EDT _____
PATH 0.1 cm _____
ORIGIN Isomet _____
SOLVENT _____
REF _____
λ SPEED: 5 nm/min _____
SCALE _____
SENS _____
PERIOD _____
SOURCE: W _____
H₂ _____
D₂ _____
20DETECTOR: PM _____
PbS _____
ANALYST: JB _____
DATE: 3/20/72 _____

Figure B3.



SAMPLE EDT _____
 PATH _____ cm
 ORIGIN Isomet
 SOLVENT _____
 REF _____
 λ SPEED: _____ nm/min
 SCALE _____
 SENS _____
 PERIOD _____
 SOURCE: W _____
 H₂ _____
 D₂ _____
 DETECTOR: PM _____
 PbS _____
 ANALYST JB _____
 DATE: 3/21/72

Copyright 1967
 Beckman Instruments, Inc.

Figure B4.

31

SPECTRUM NO. _____
DATE June 7, 1972

SAMPLE Ethylene Diamine Tartrate

SOURCE Leomet Cells

STRUCTURE _____
IR-20 transmission at normal incidence.

PATH 1.35 mm

CONCENTRATION _____

PHASE _____

COMMENTS _____

ANALYST AWB

Beckman

INFRARED

SPECTROPHOTOMETER

SPECTRUM NO. _____

DATE _____

SAMPLE EDT

Ethylene Diamine Tartrate

SOURCE Isomet

STRUCTURE _____

IR-20 specular reflectance at 30° incidence

PATH _____ mm

CONCENTRATION _____

PHASE _____

COMMENTS _____

ANALYST _____

Beckman

INFRARED

SPECTROPHOTOMETER

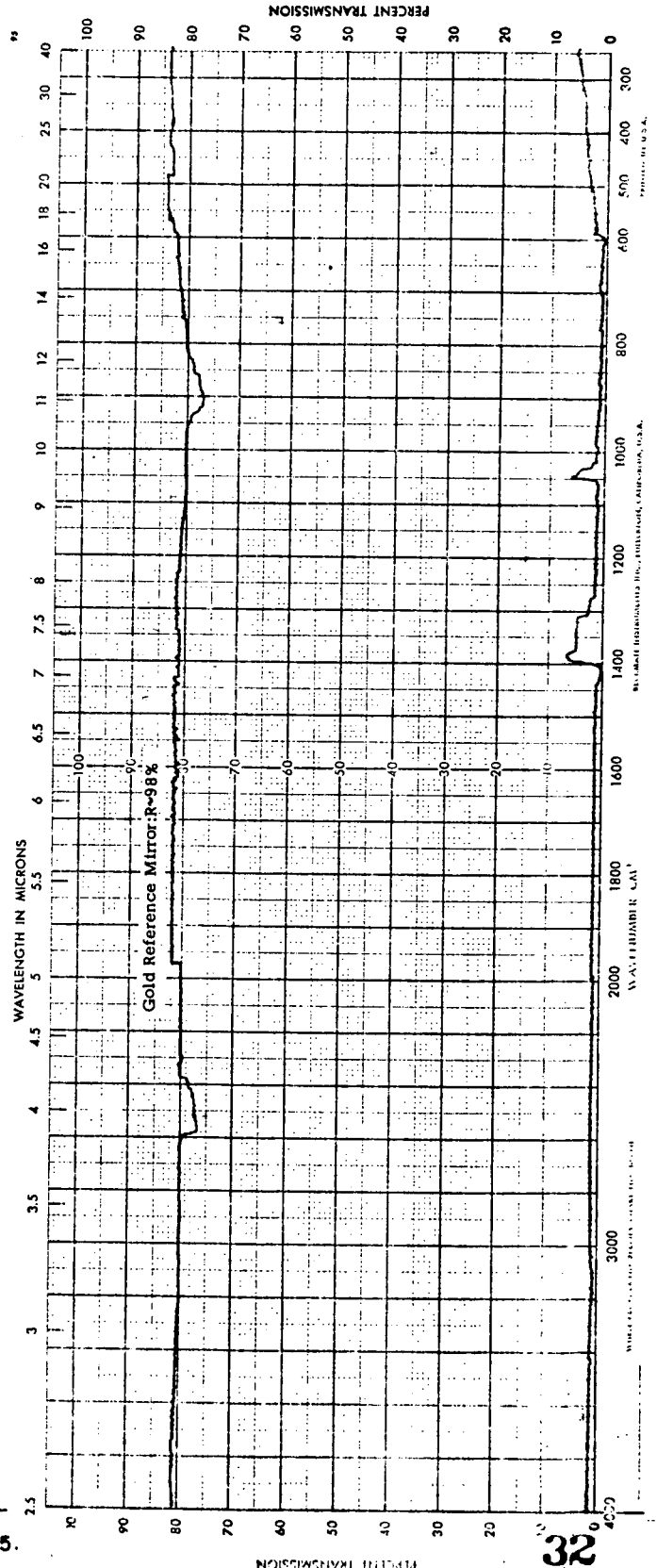
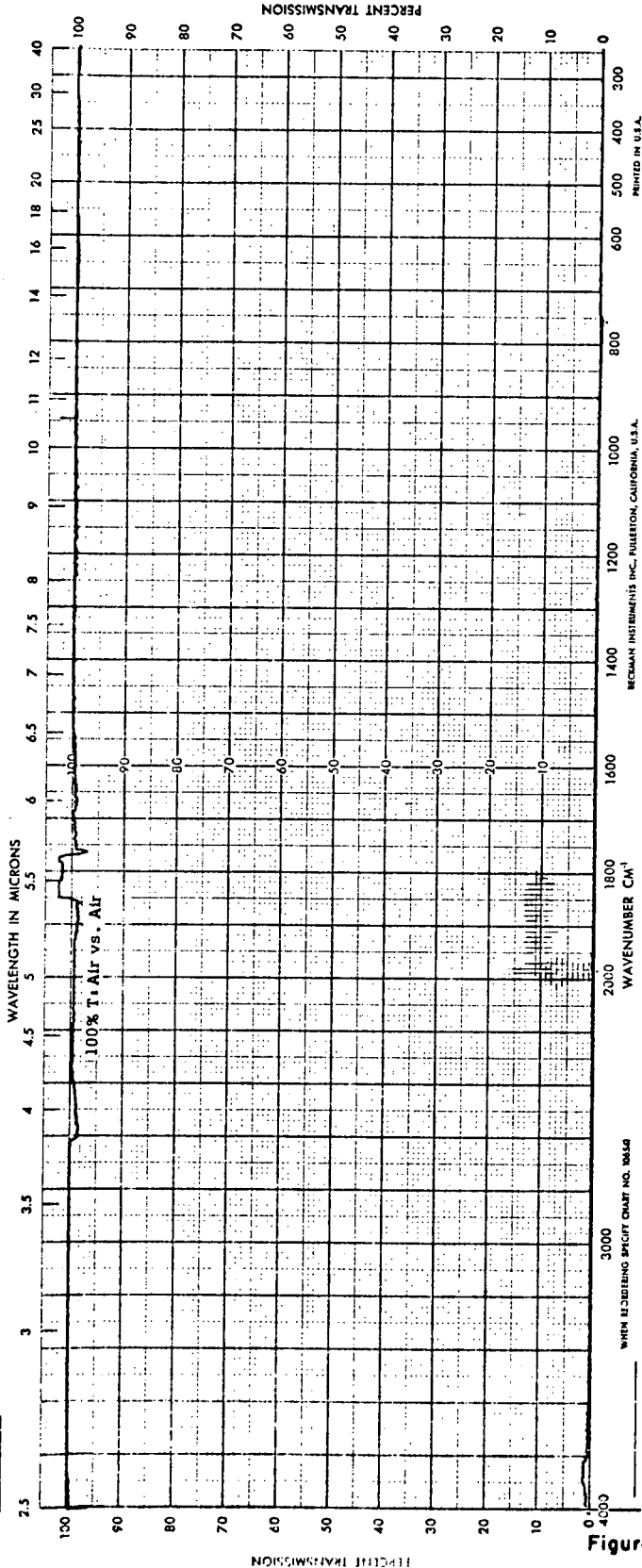
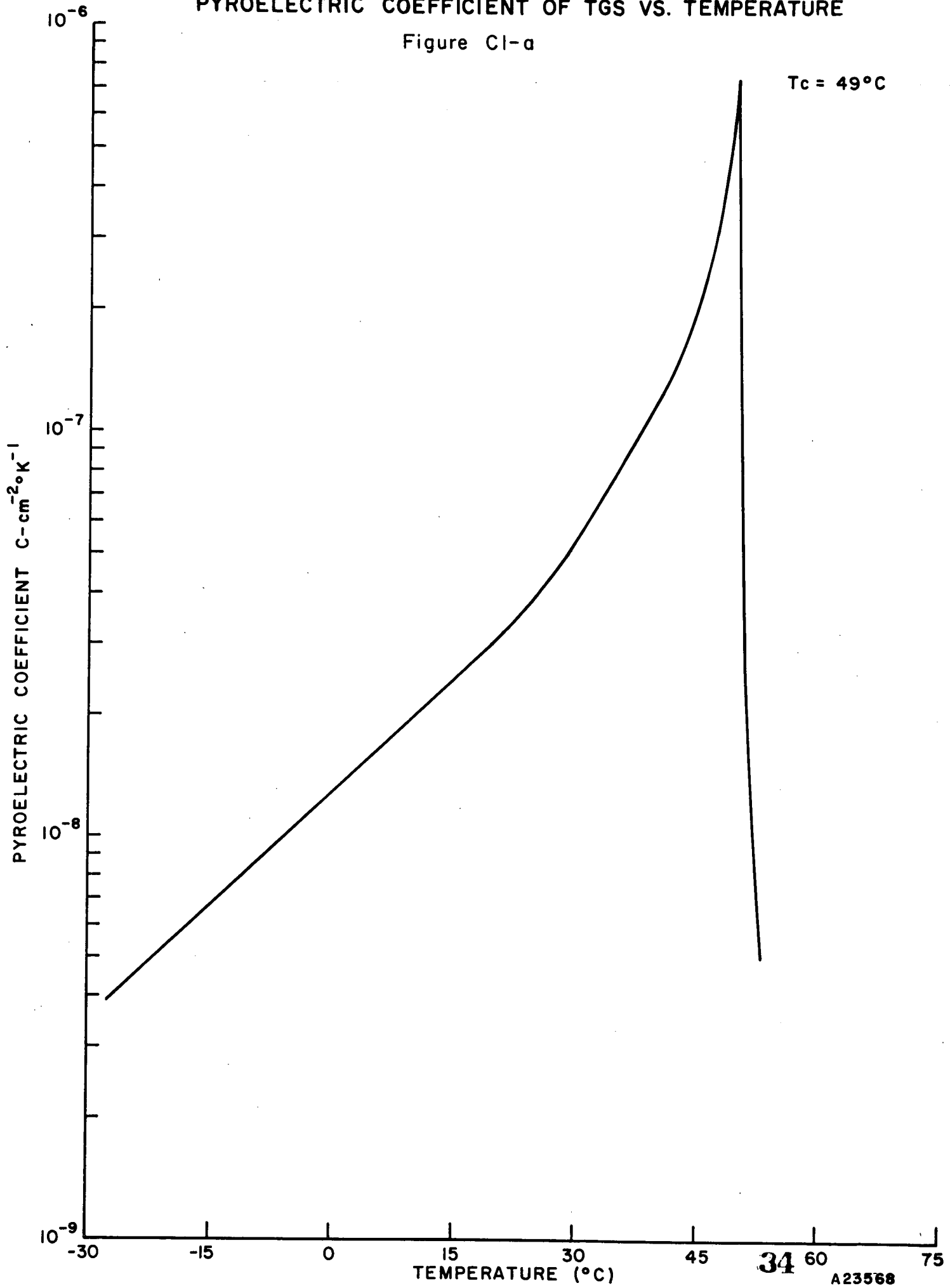


Figure 85.

APPENDIX C - PYROELECTRIC COEFFICIENT, DIELECTRIC CONSTANT, AND LOSS
TANGENT CURVES OF SELECTED PYROELECTRIC MATERIALS

PYROELECTRIC COEFFICIENT OF TGS VS. TEMPERATURE

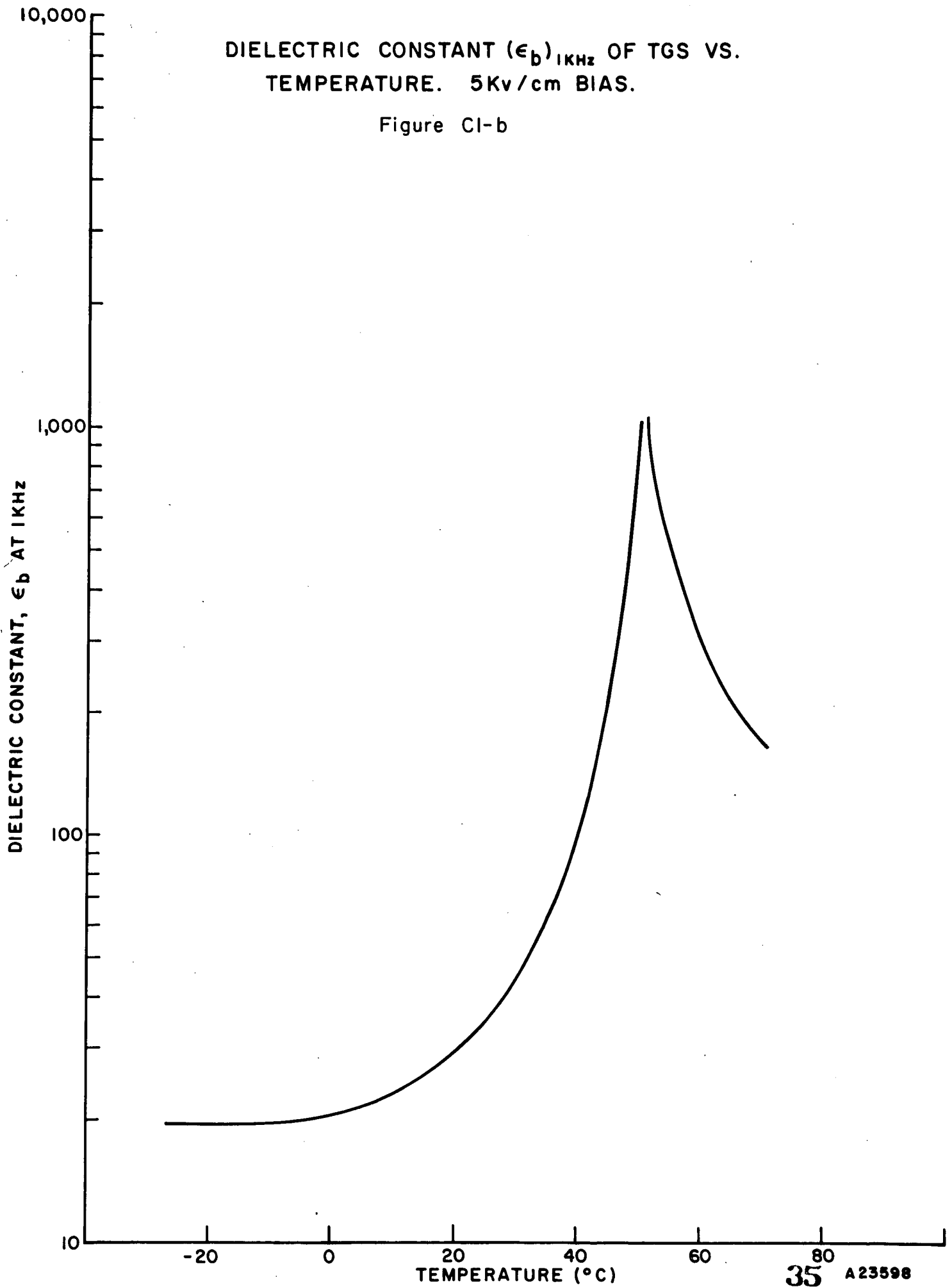
Figure C1-a



T_c = 49°C

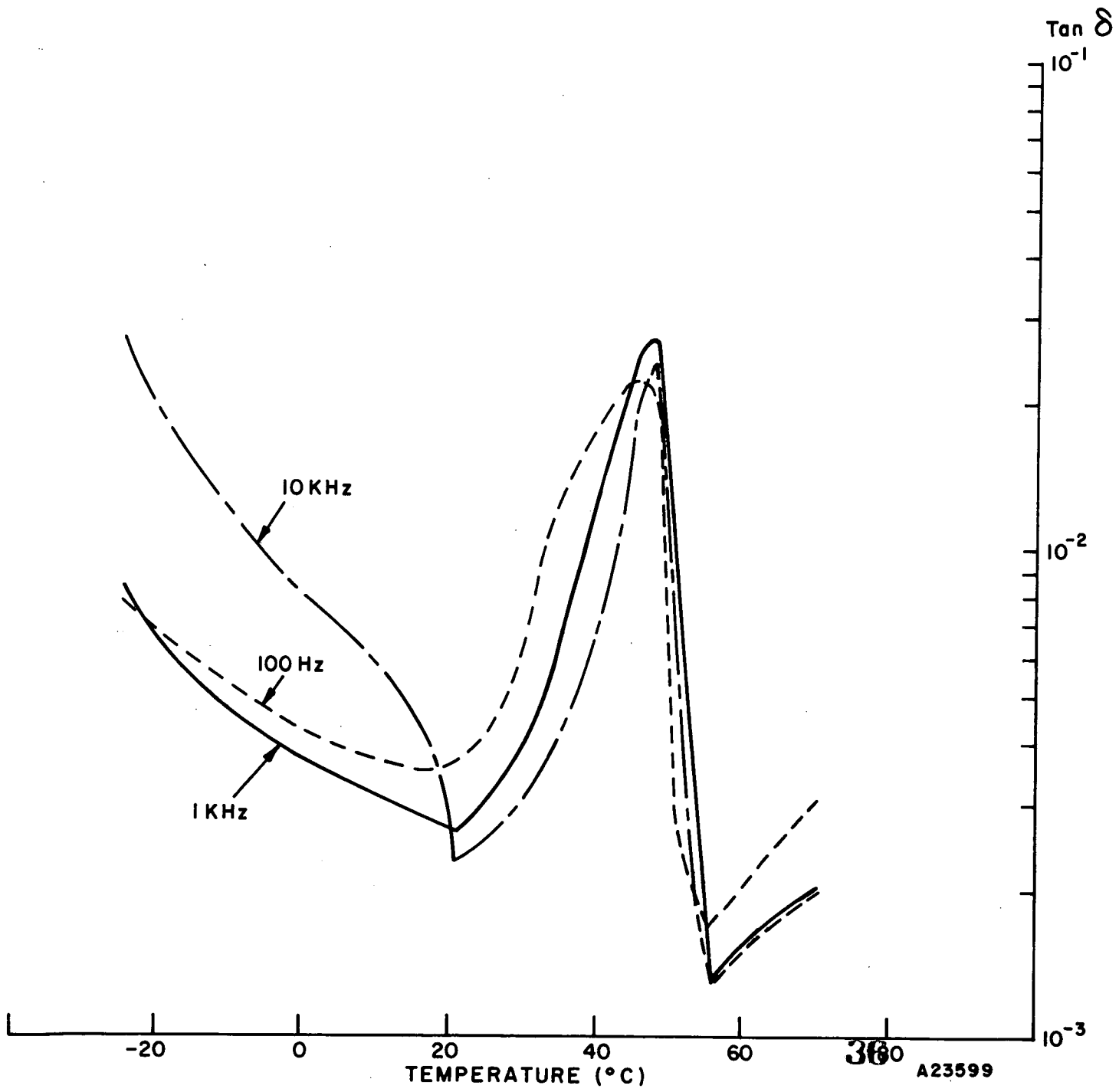
DIELECTRIC CONSTANT (ϵ_b)_{1KHz} OF TGS VS.
TEMPERATURE. 5Kv/cm BIAS.

Figure CI-b



LOSS TANGENT OF TGS VS. TEMPERATURE. 5Kv/cm BIAS

Figure Cl-c

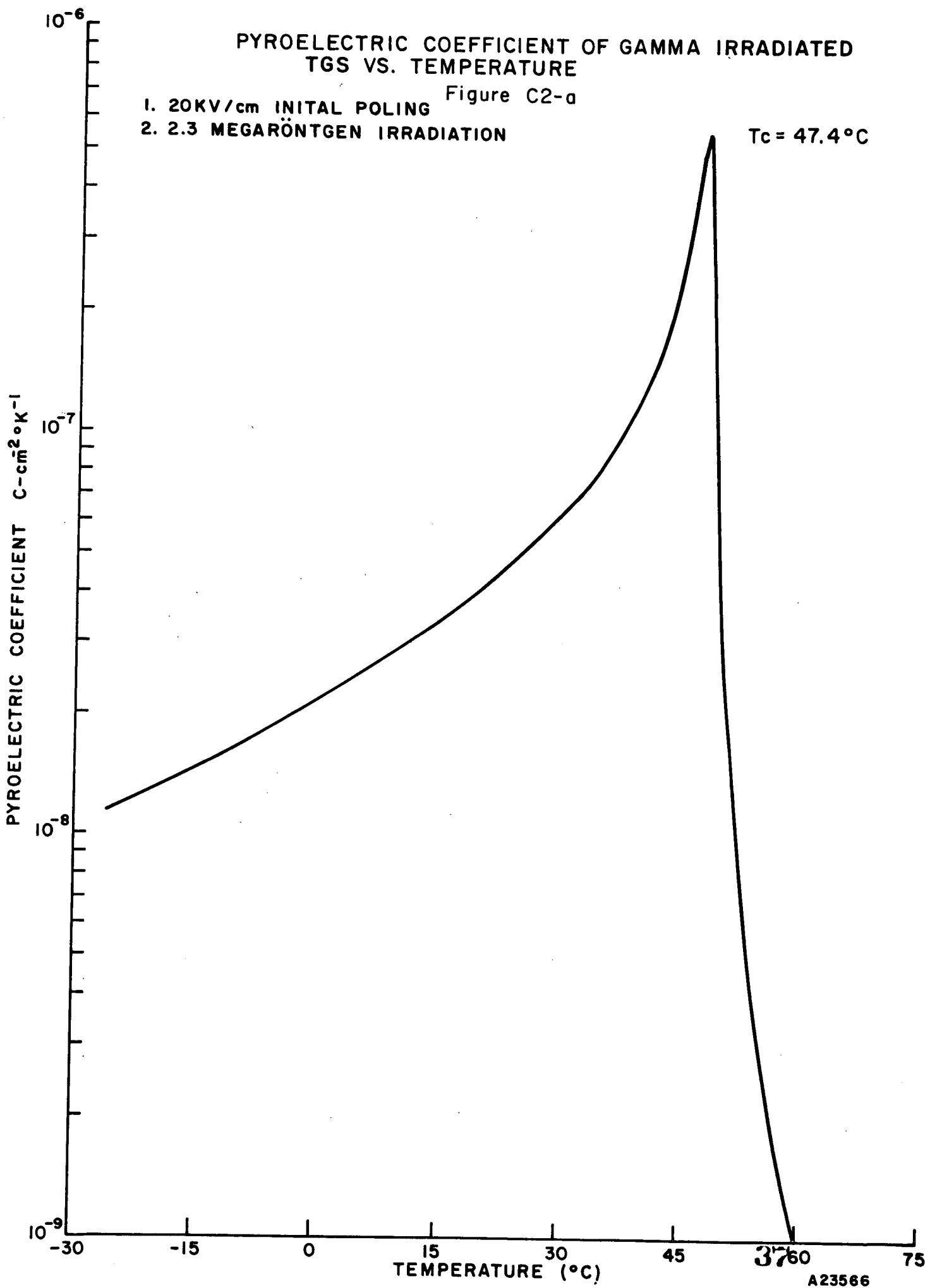


PYROELECTRIC COEFFICIENT OF GAMMA IRRADIATED
TGS VS. TEMPERATURE

Figure C2-a

- 1. 20KV/cm INITIAL POLING
- 2. 2.3 MEGARÖNTGEN IRRADIATION

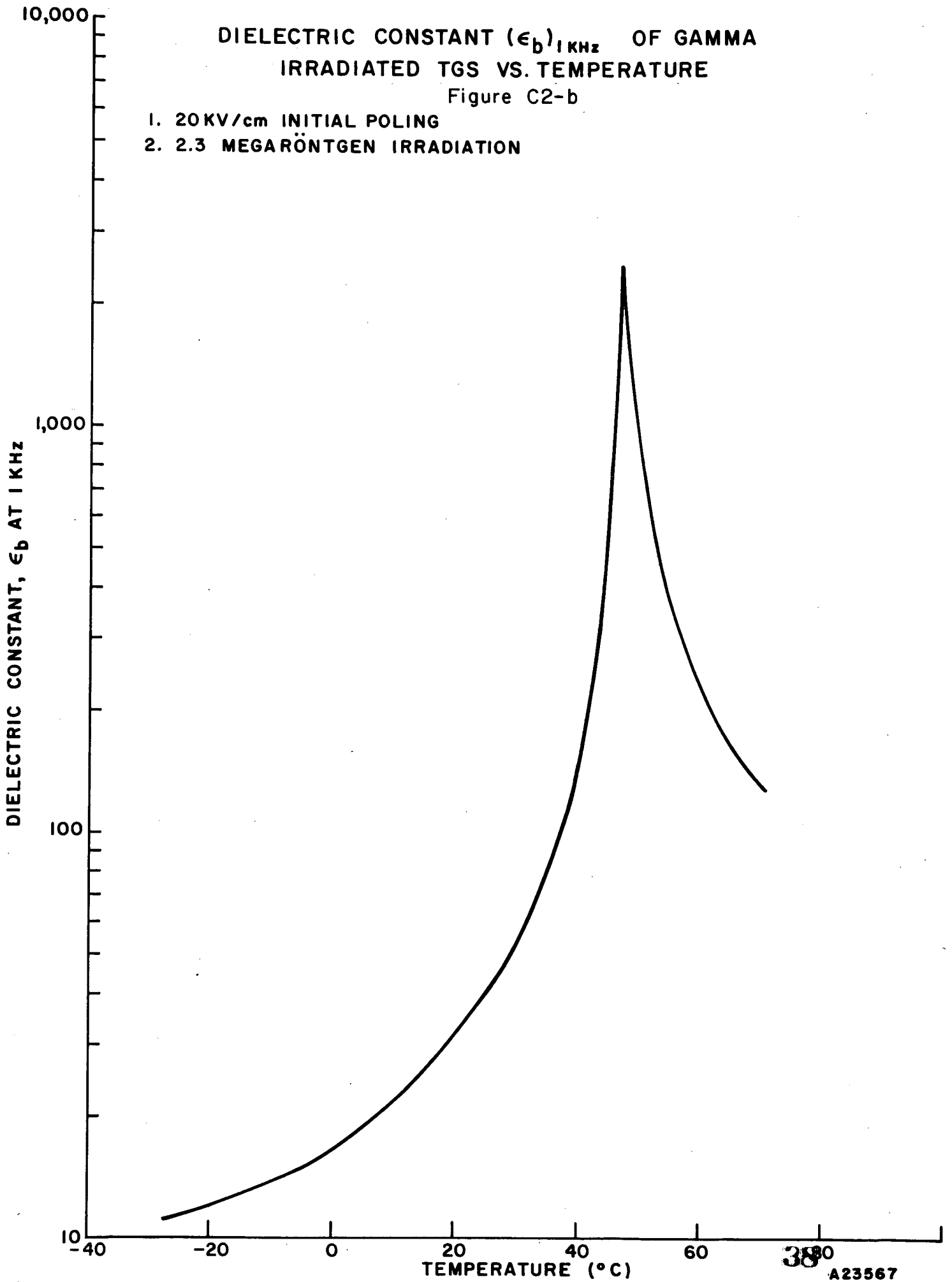
T_c = 47.4°C



DIELECTRIC CONSTANT (ϵ_b)_{1 KHz} OF GAMMA
IRRADIATED TGS VS. TEMPERATURE

Figure C2-b

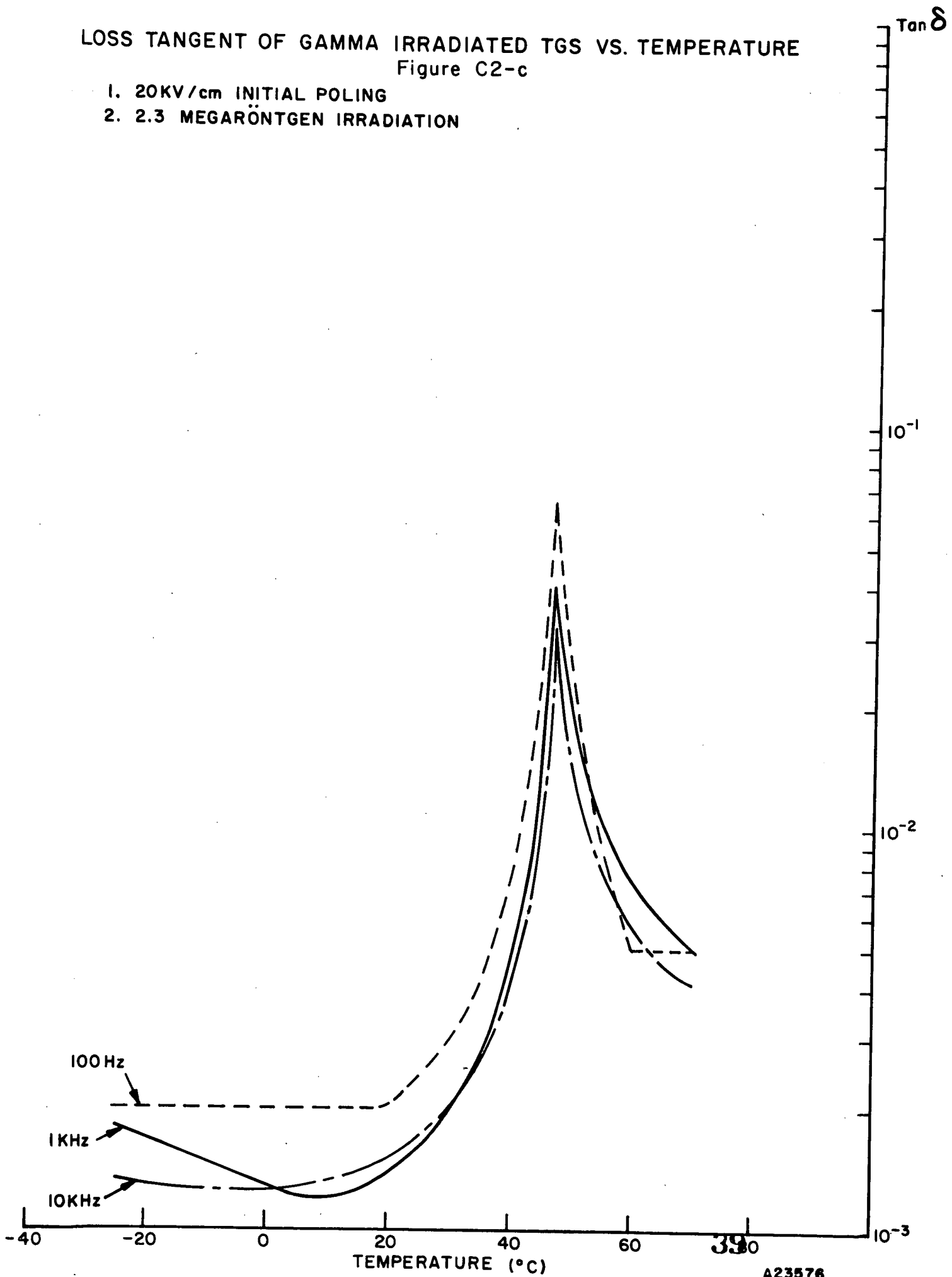
1. 20KV/cm INITIAL POLING
2. 2.3 MEGARÖNTGEN IRRADIATION



LOSS TANGENT OF GAMMA IRRADIATED TGS VS. TEMPERATURE

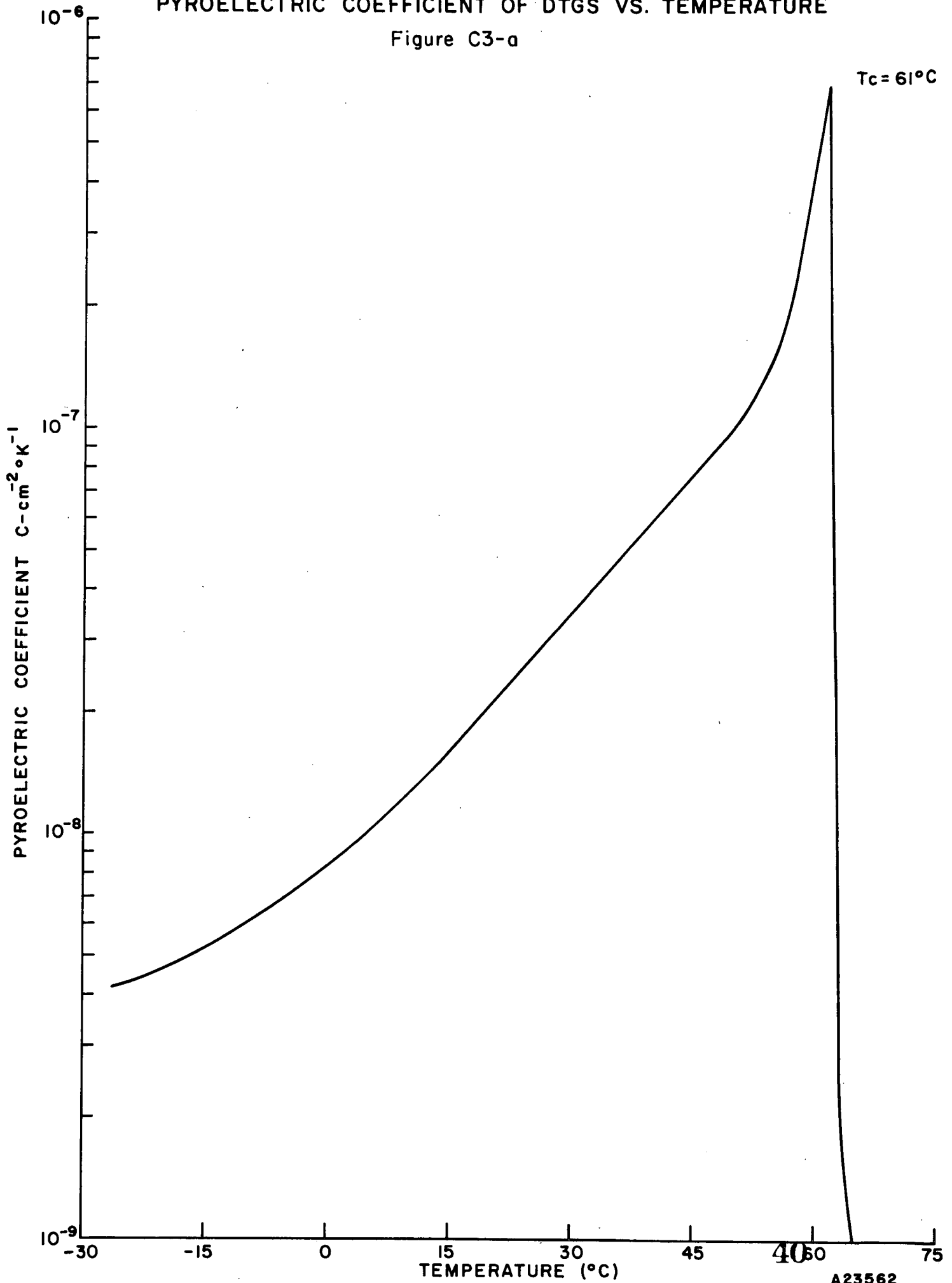
Figure C2-c

- 1. 20KV/cm INITIAL POLING
- 2. 2.3 MEGARÖNTGEN IRRADIATION



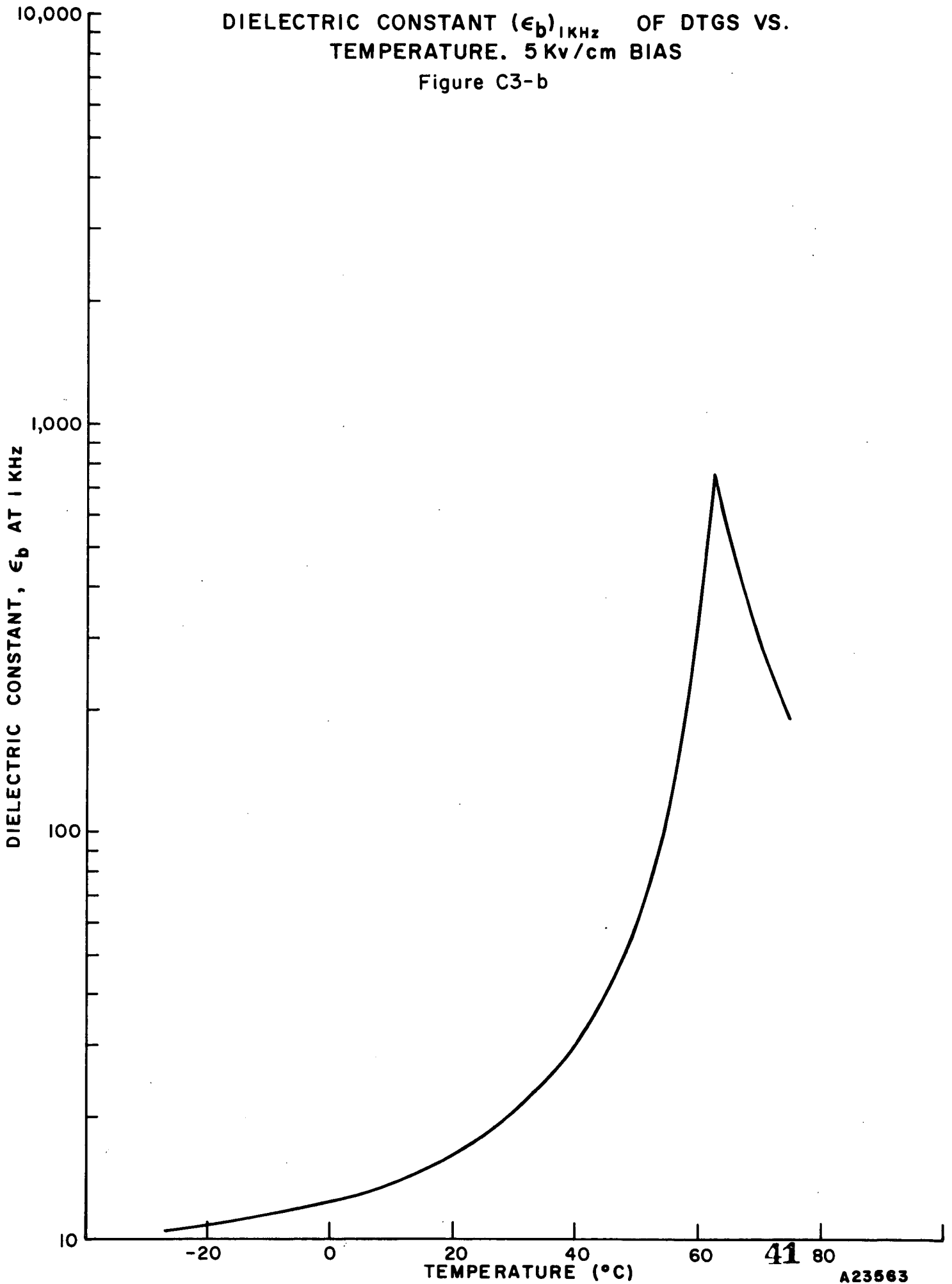
PYROELECTRIC COEFFICIENT OF DTGS VS. TEMPERATURE

Figure C3-a



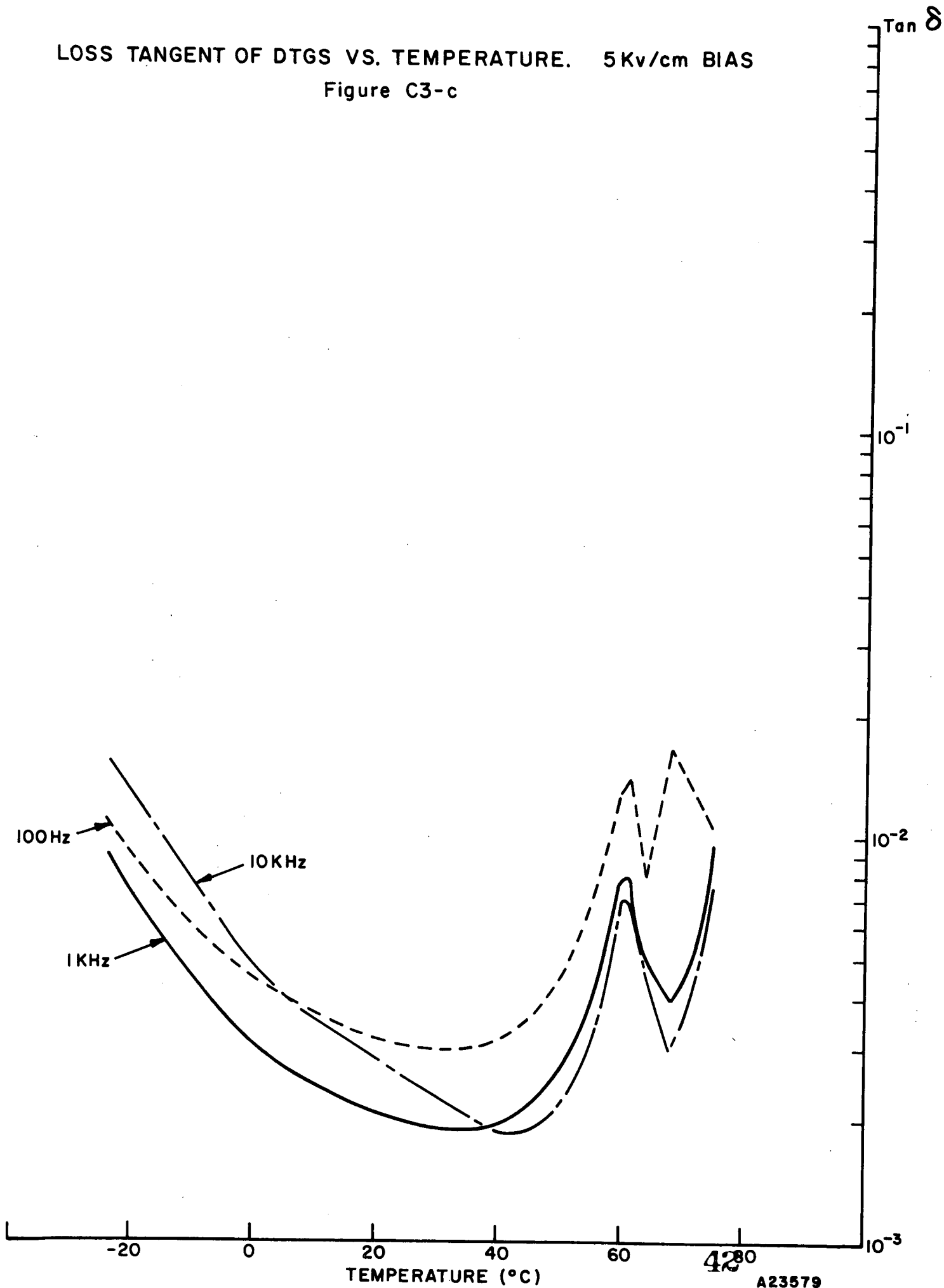
DIELECTRIC CONSTANT (ϵ_b)_{1KHz} OF DTGS VS.
TEMPERATURE. 5 Kv/cm BIAS

Figure C3-b



LOSS TANGENT OF DTGS VS. TEMPERATURE. 5 Kv/cm BIAS

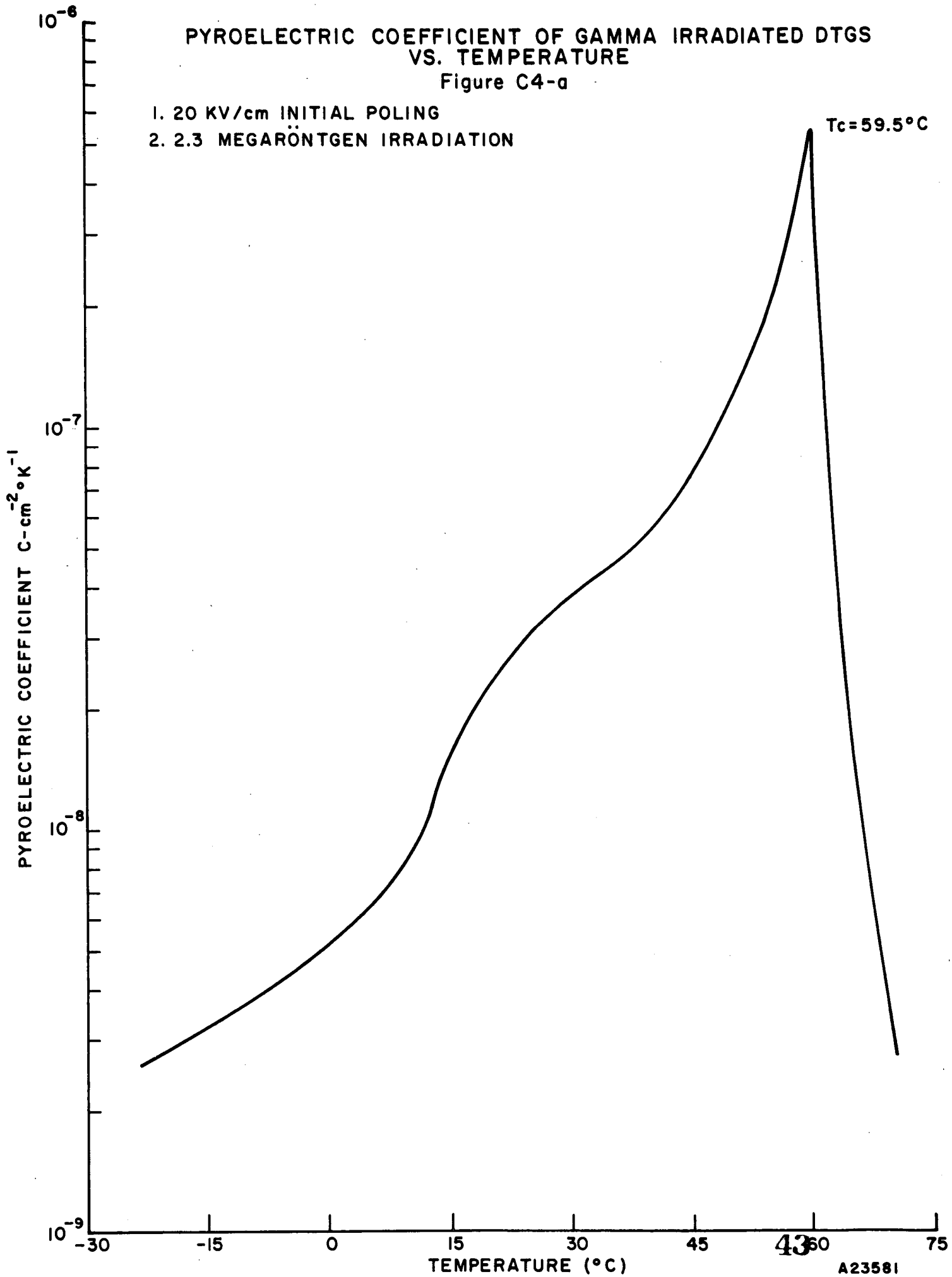
Figure C3-c



PYROELECTRIC COEFFICIENT OF GAMMA IRRADIATED DTGS
VS. TEMPERATURE

Figure C4-a

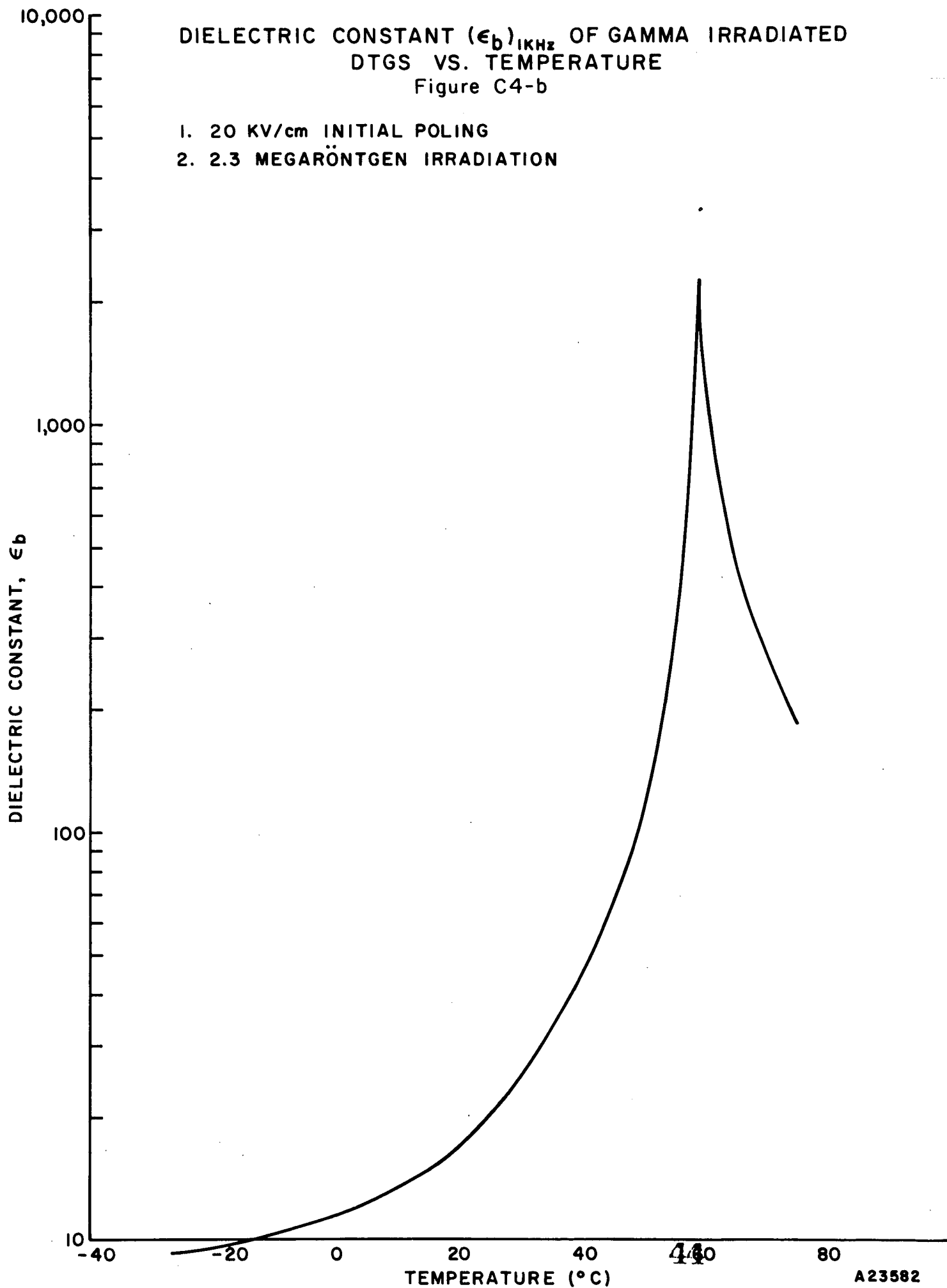
- 1. 20 KV/cm INITIAL POLING
- 2. 2.3 MEGARÖNTGEN IRRADIATION



DIELECTRIC CONSTANT (ϵ_b)_{1KHz} OF GAMMA IRRADIATED
DTGS VS. TEMPERATURE

Figure C4-b

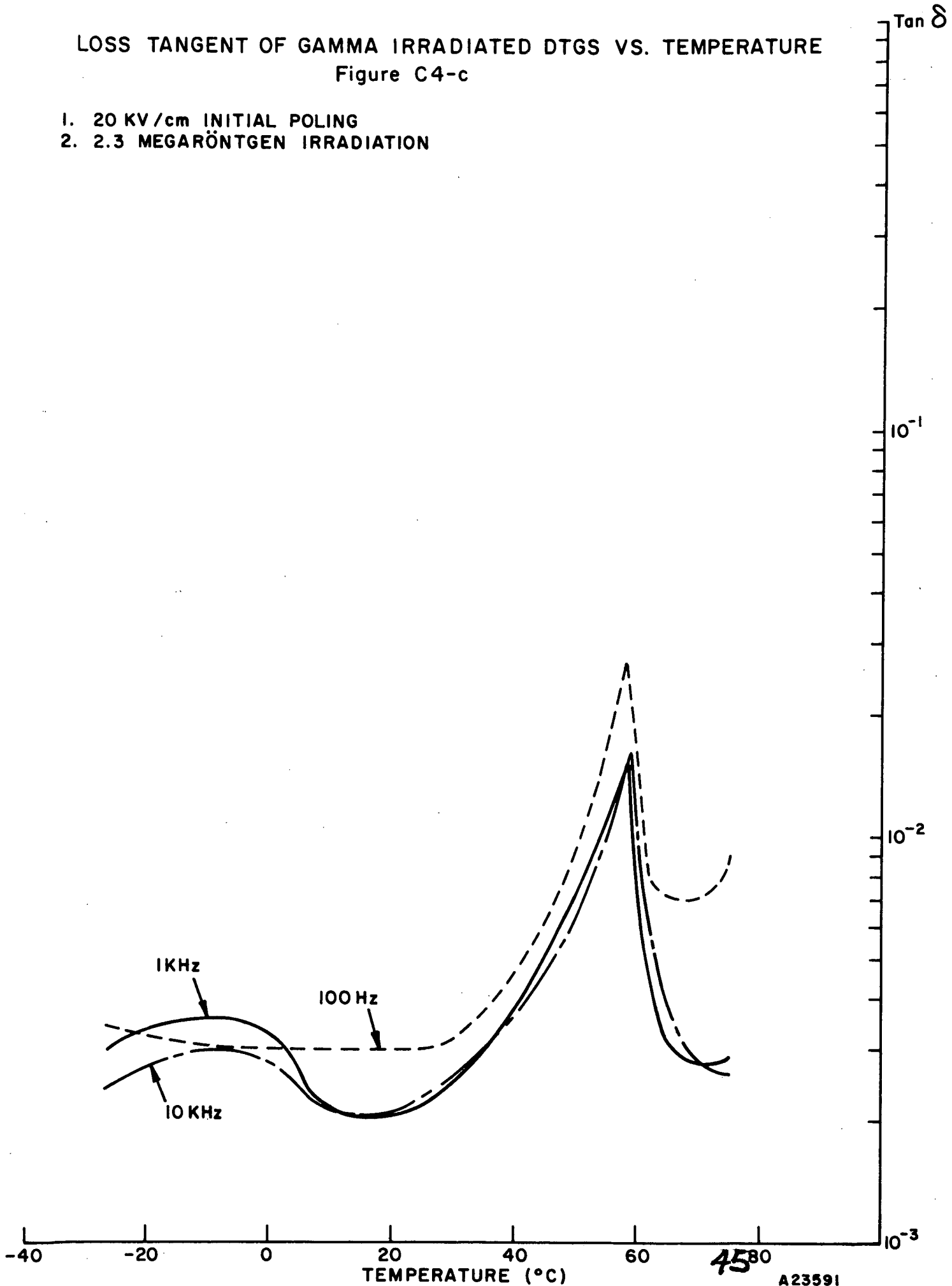
1. 20 KV/cm INITIAL POLING
2. 2.3 MEGARÖNTGEN IRRADIATION



LOSS TANGENT OF GAMMA IRRADIATED DTGS VS. TEMPERATURE

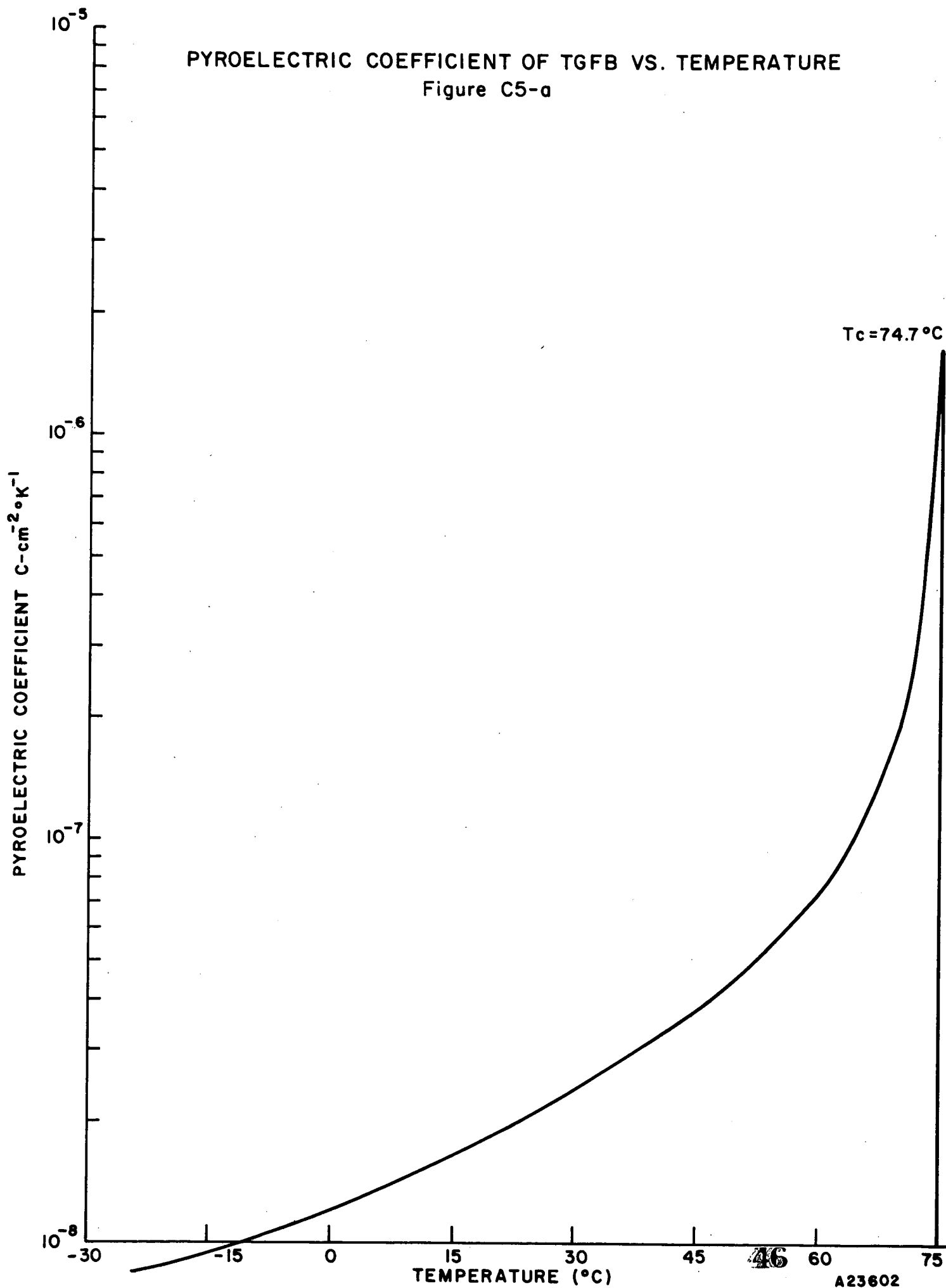
Figure C4-c

- 1. 20 KV/cm INITIAL POLING
- 2. 2.3 MEGARÖNTGEN IRRADIATION



PYROELECTRIC COEFFICIENT OF TGFB VS. TEMPERATURE

Figure C5-a



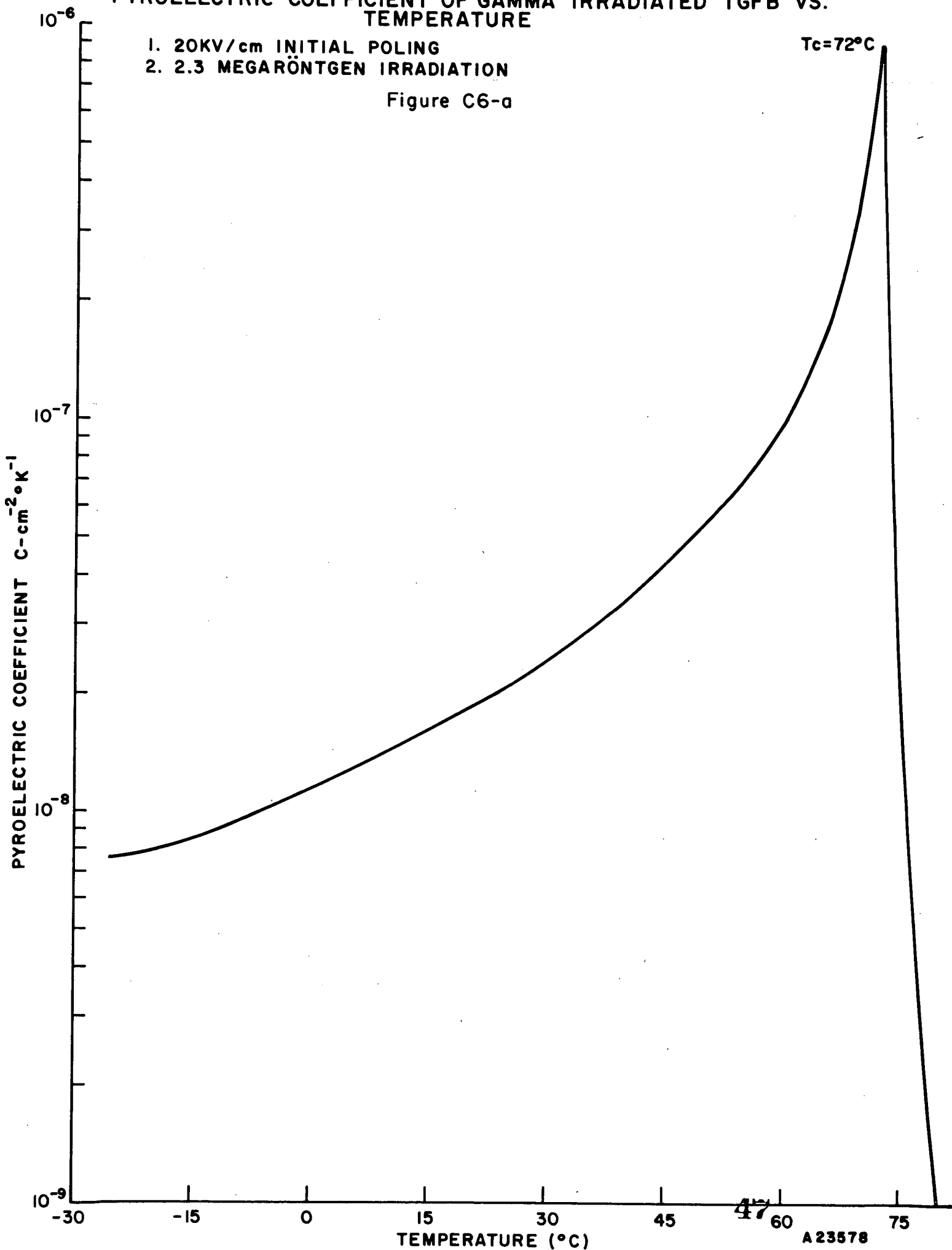
46

PYROELECTRIC COEFFICIENT OF GAMMA IRRADIATED TGFB VS. TEMPERATURE

- 1. 20KV/cm INITIAL POLING
- 2. 2.3 MEGARÖNTGEN IRRADIATION

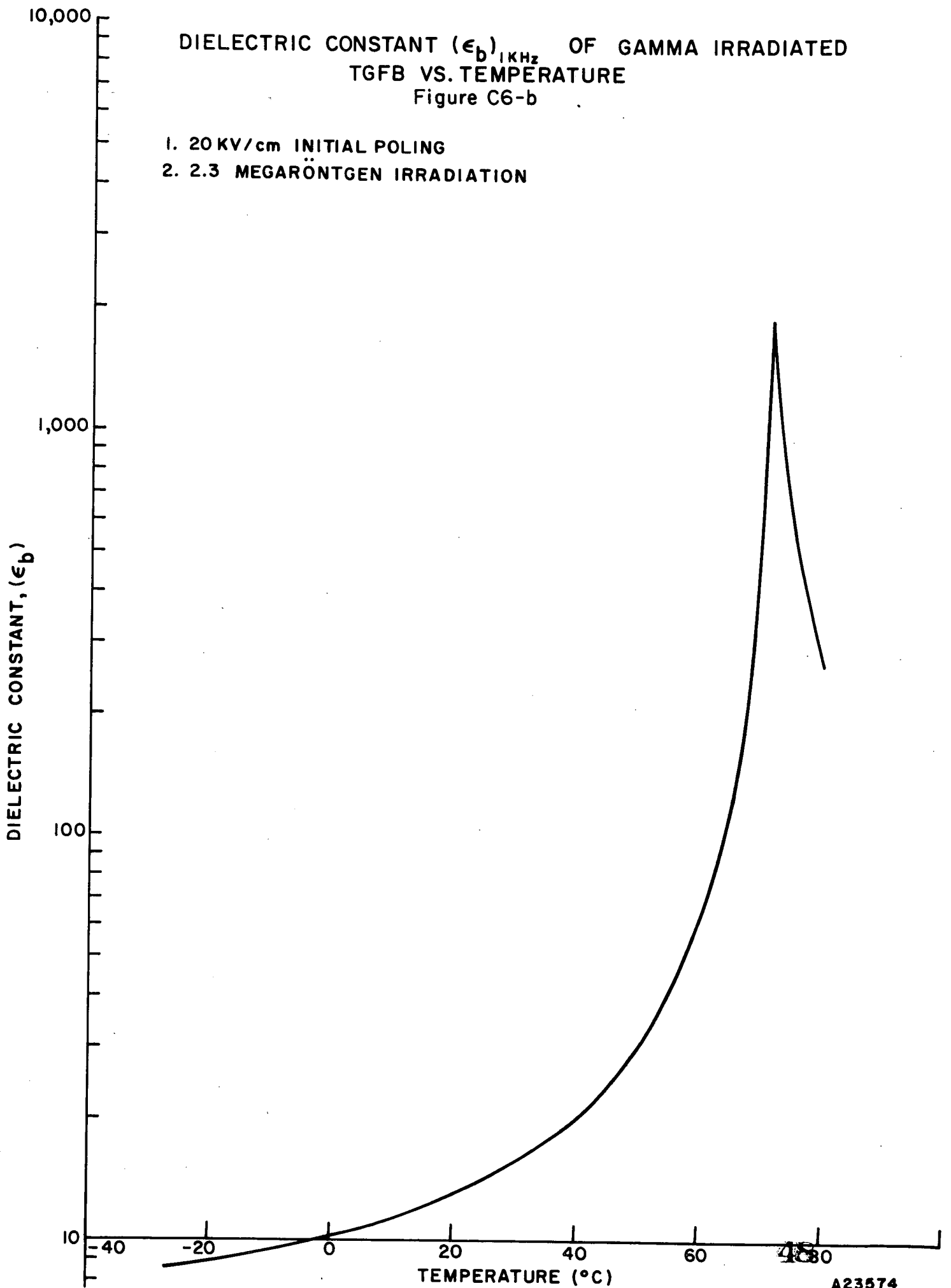
Figure C6-a

Tc=72°C



DIELECTRIC CONSTANT (ϵ_b)_{1KHz} OF GAMMA IRRADIATED
TGFB VS. TEMPERATURE
Figure C6-b

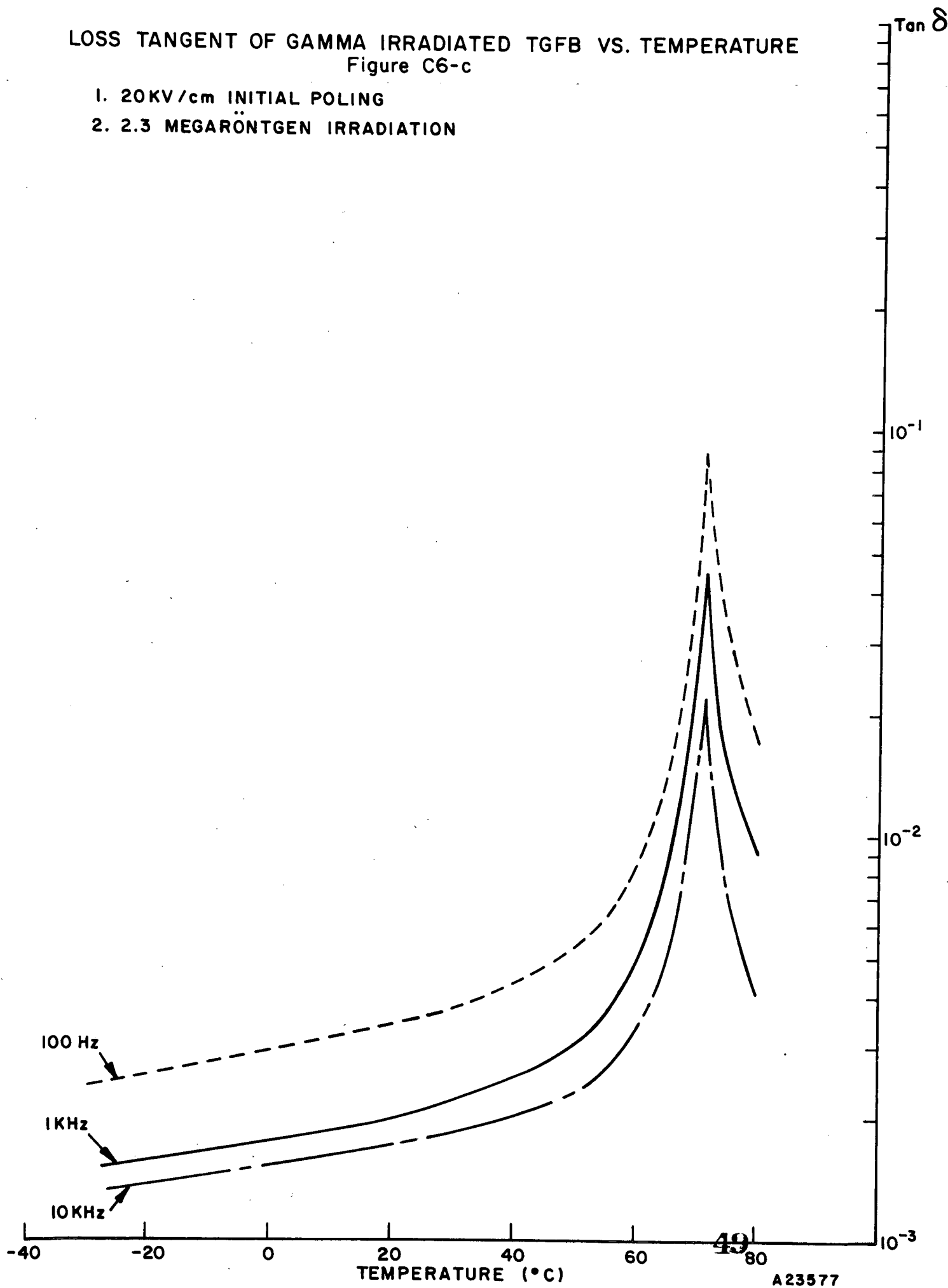
1. 20 KV/cm INITIAL POLING
2. 2.3 MEGARÖNTGEN IRRADIATION



LOSS TANGENT OF GAMMA IRRADIATED TGFB VS. TEMPERATURE

Figure C6-c

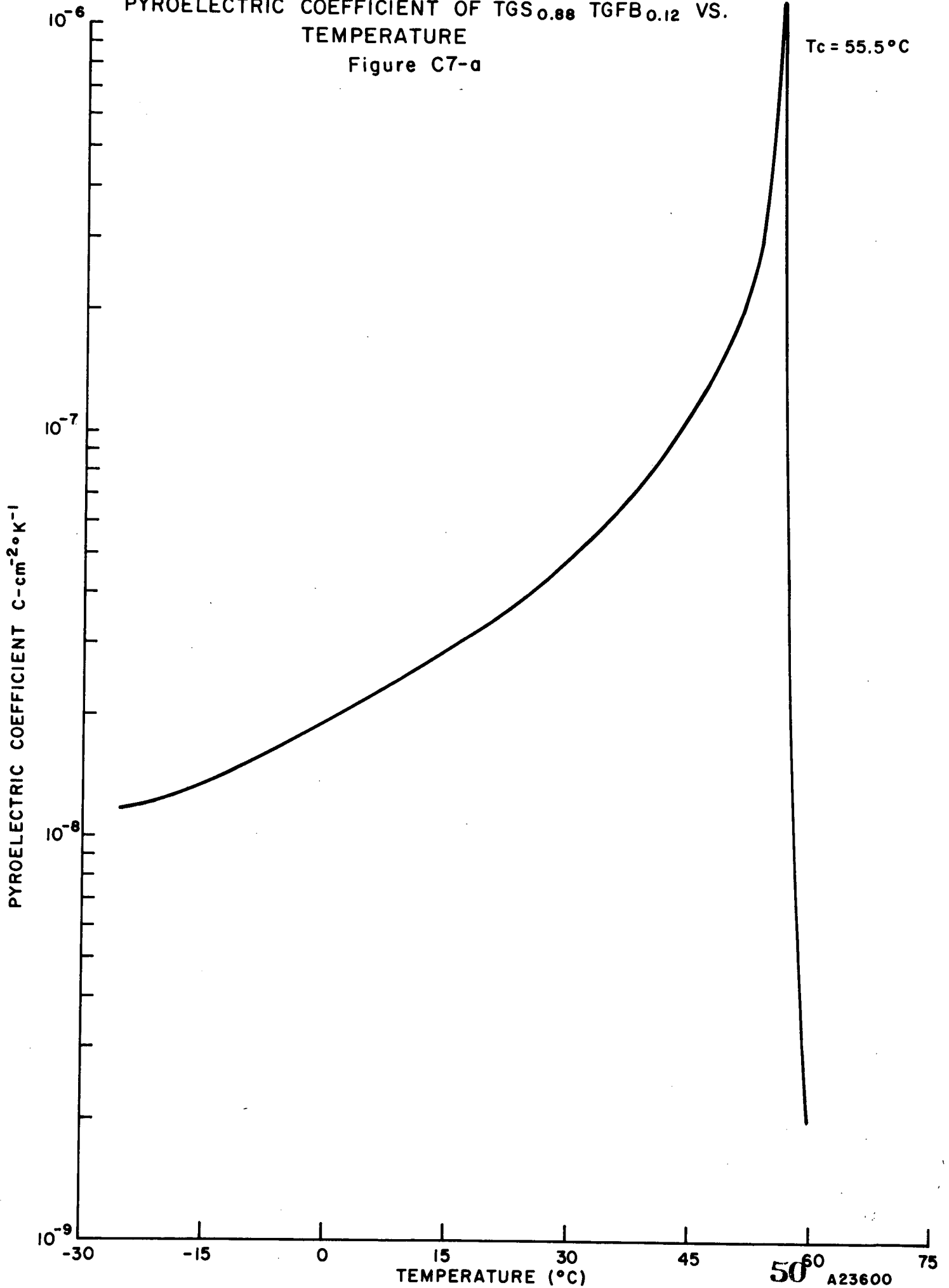
- 1. 20KV/cm INITIAL POLING
- 2. 2.3 MEGARÖNTGEN IRRADIATION



PYROELECTRIC COEFFICIENT OF TGS_{0.88} TGFB_{0.12} VS. TEMPERATURE

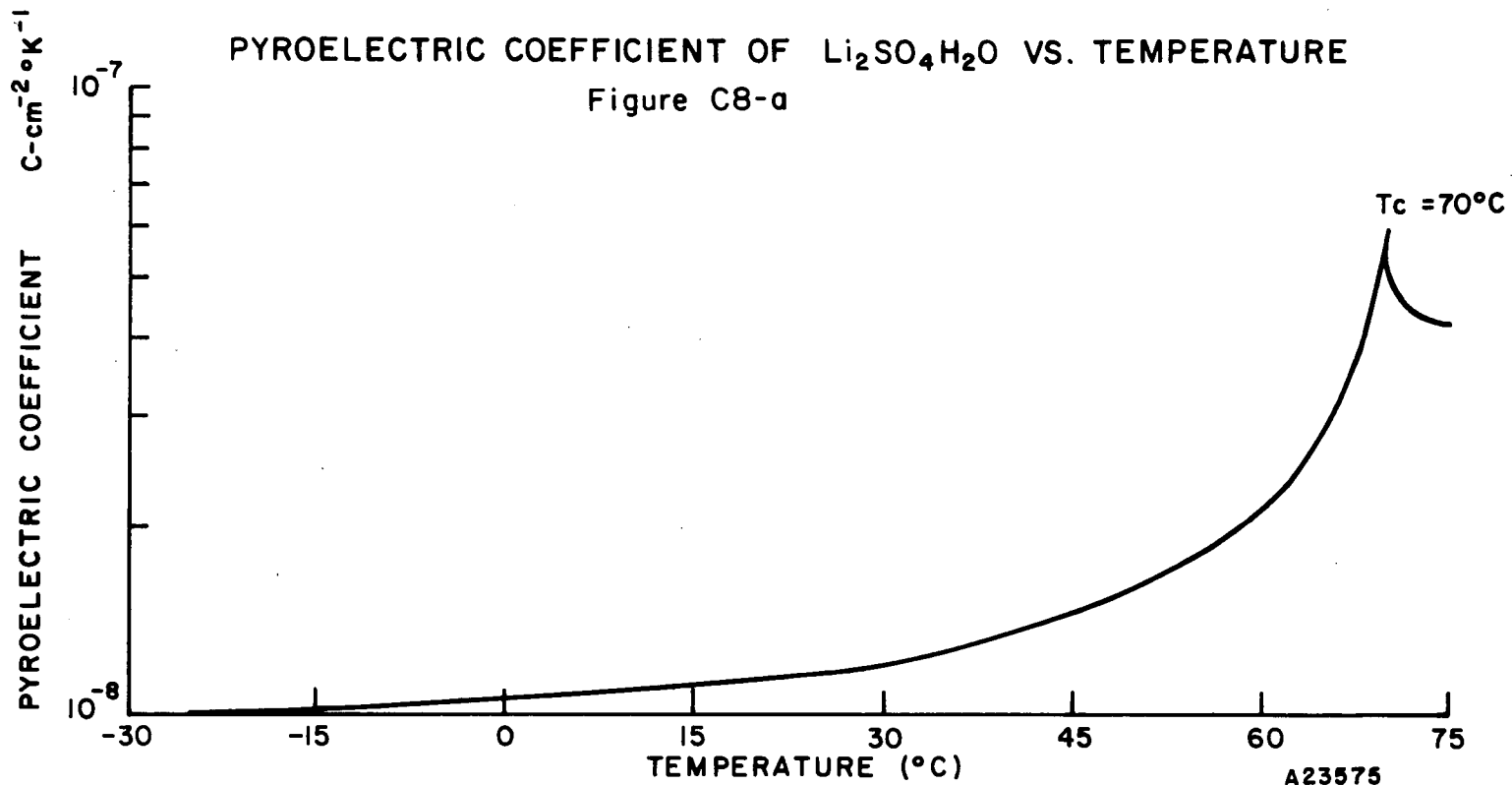
Figure C7-a

T_c = 55.5°C



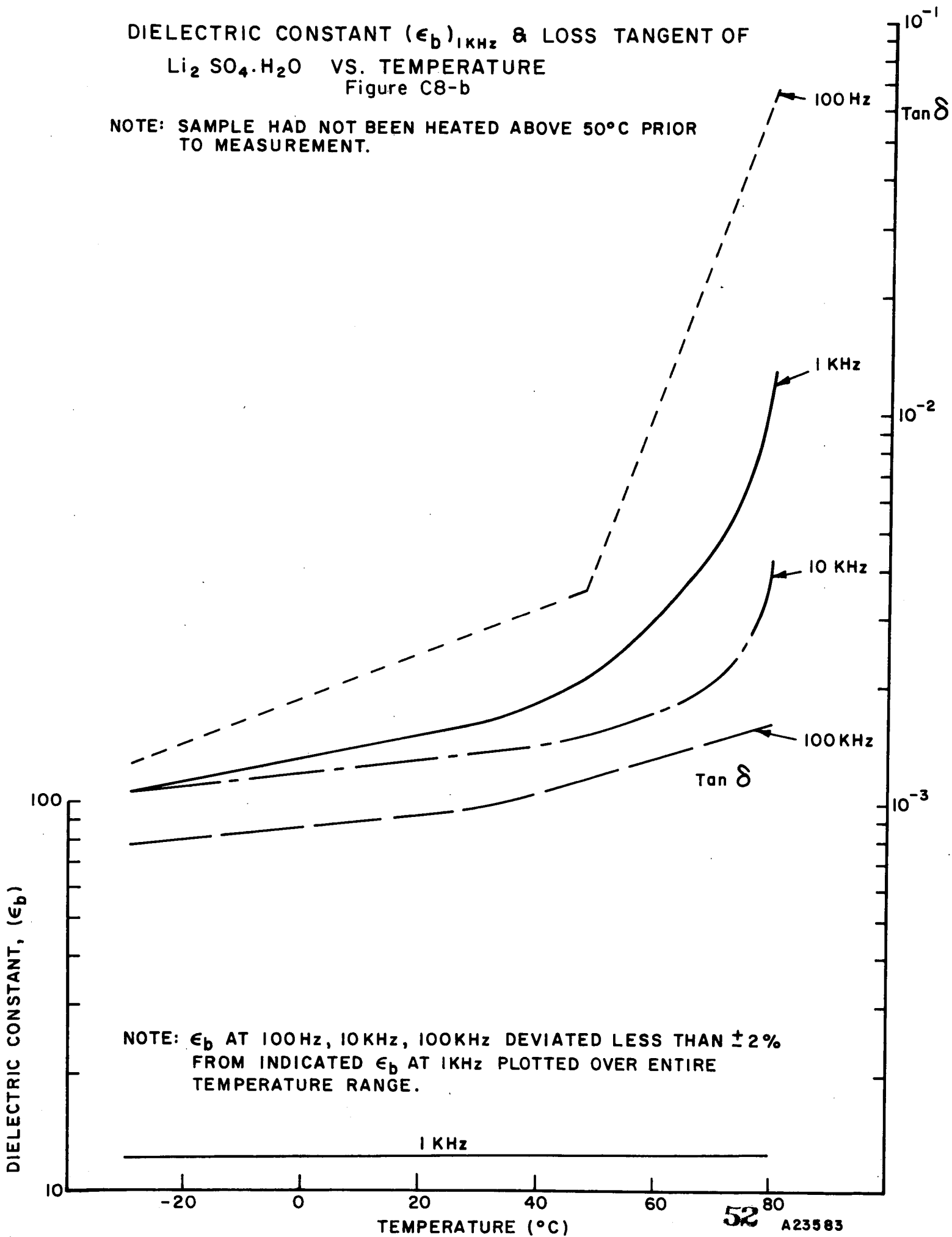
PYROELECTRIC COEFFICIENT OF $\text{Li}_2\text{SO}_4\cdot\text{H}_2\text{O}$ VS. TEMPERATURE

Figure C8-a



DIELECTRIC CONSTANT (ϵ_b)_{1KHz} & LOSS TANGENT OF
 $\text{Li}_2\text{SO}_4 \cdot \text{H}_2\text{O}$ VS. TEMPERATURE
 Figure C8-b

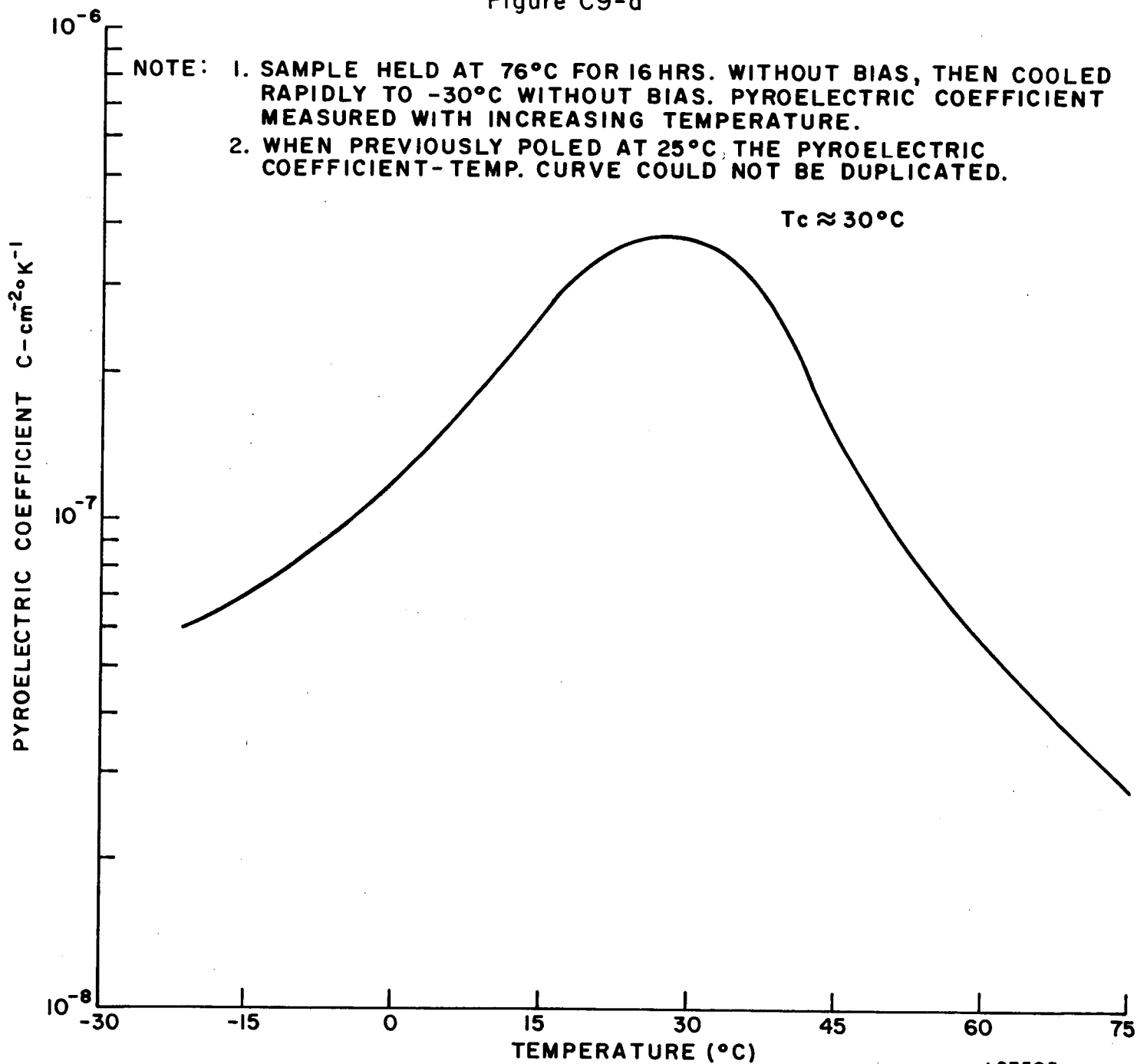
NOTE: SAMPLE HAD NOT BEEN HEATED ABOVE 50°C PRIOR TO MEASUREMENT.



NOTE: ϵ_b AT 100Hz, 10KHz, 100KHz DEVIATED LESS THAN $\pm 2\%$ FROM INDICATED ϵ_b AT 1KHz PLOTTED OVER ENTIRE TEMPERATURE RANGE.

PYROELECTRIC COEFFICIENT OF $\text{Sr}_{1-x}\text{Ba}_x\text{Nb}_2\text{O}_6$
($x=0.25$) VS. TEMPERATURE

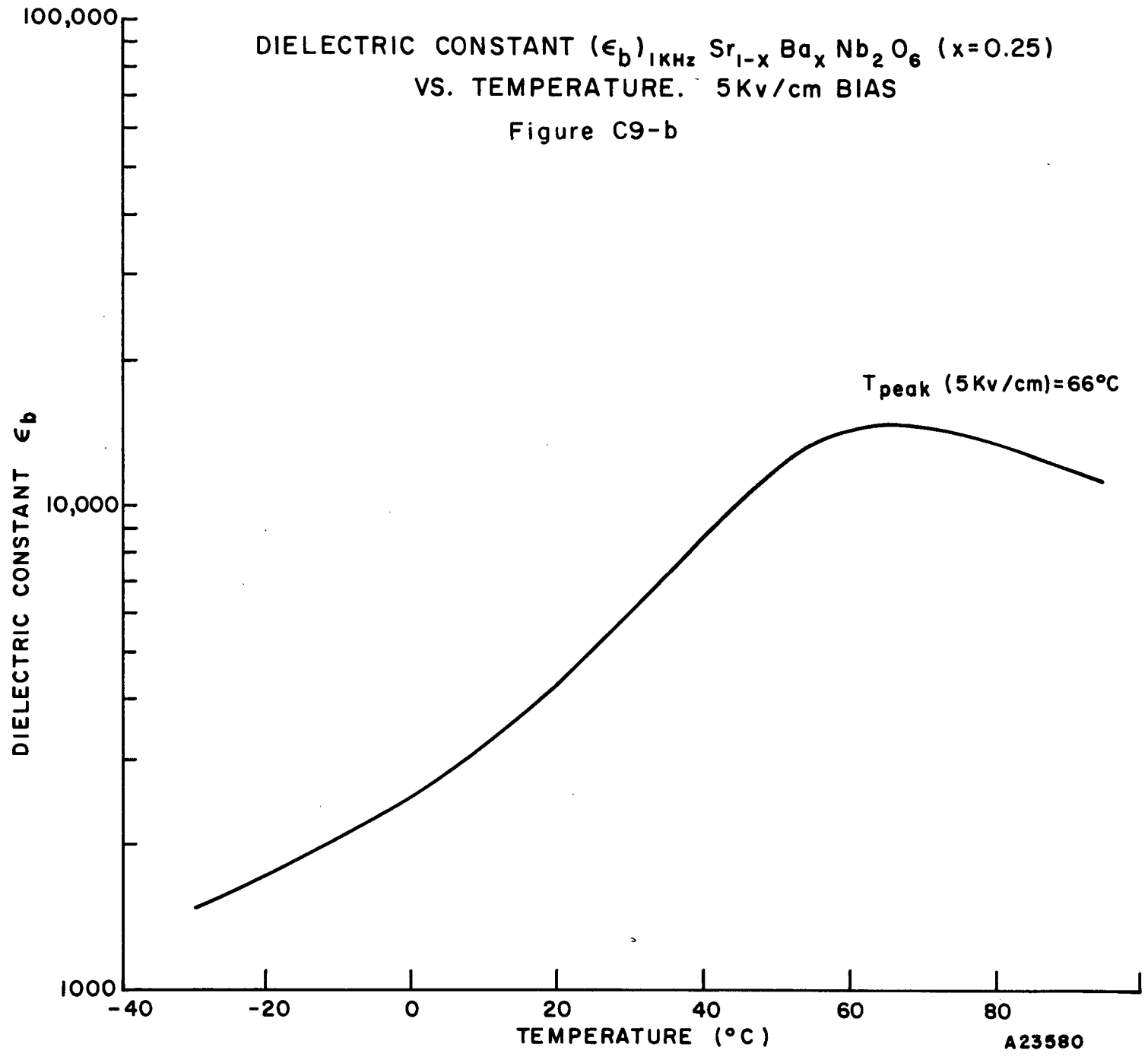
Figure C9-a



A23595

DIELECTRIC CONSTANT (ϵ_b)_{1KHz} $Sr_{1-x}Ba_xNb_2O_6$ ($x=0.25$)
VS. TEMPERATURE. 5Kv/cm BIAS

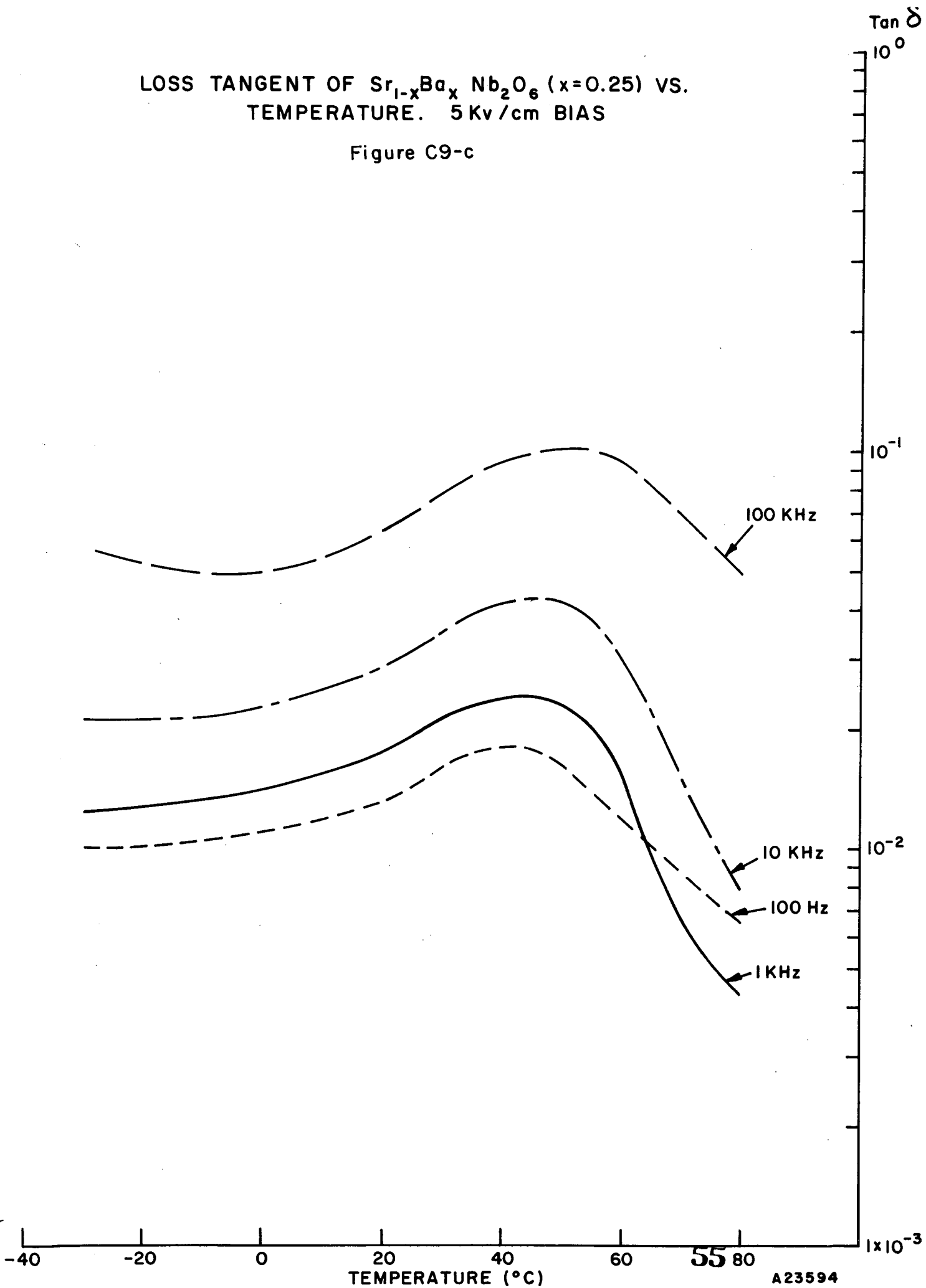
Figure C9-b



A23580

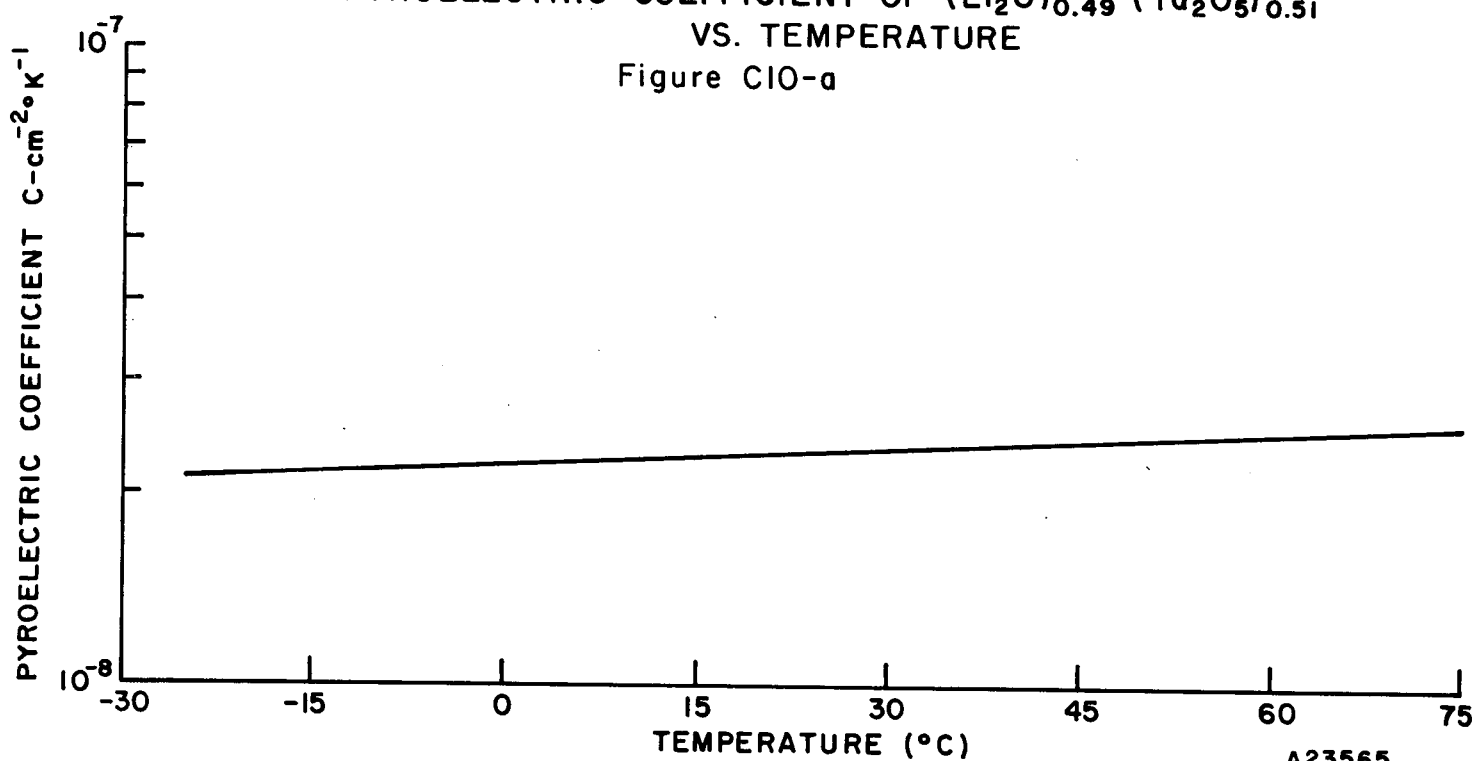
LOSS TANGENT OF $\text{Sr}_{1-x}\text{Ba}_x\text{Nb}_2\text{O}_6$ ($x=0.25$) VS.
TEMPERATURE. 5 Kv/cm BIAS

Figure C9-c



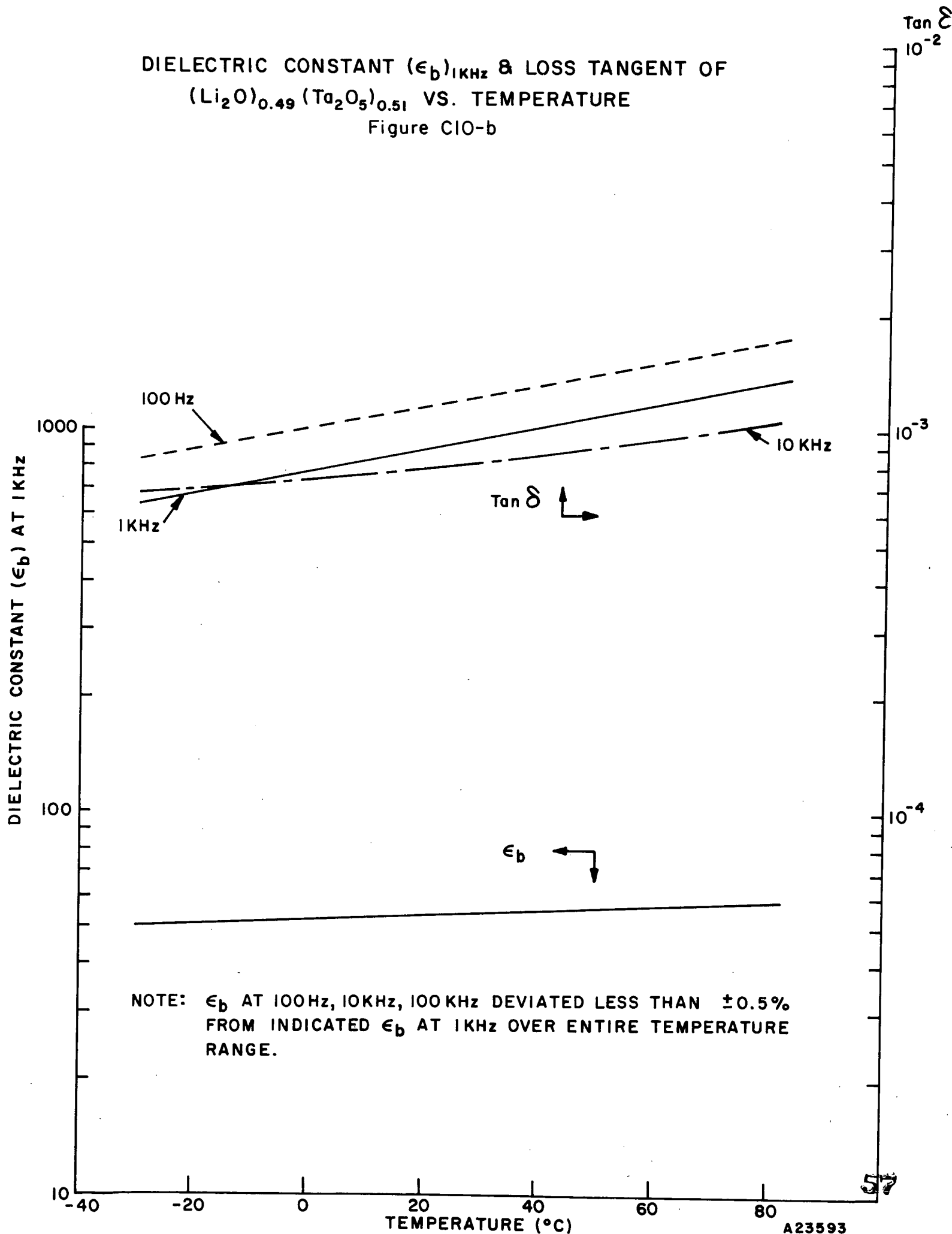
PYROELECTRIC COEFFICIENT OF $(\text{Li}_2\text{O})_{0.49} (\text{Ta}_2\text{O}_5)_{0.51}$
VS. TEMPERATURE

Figure C10-a



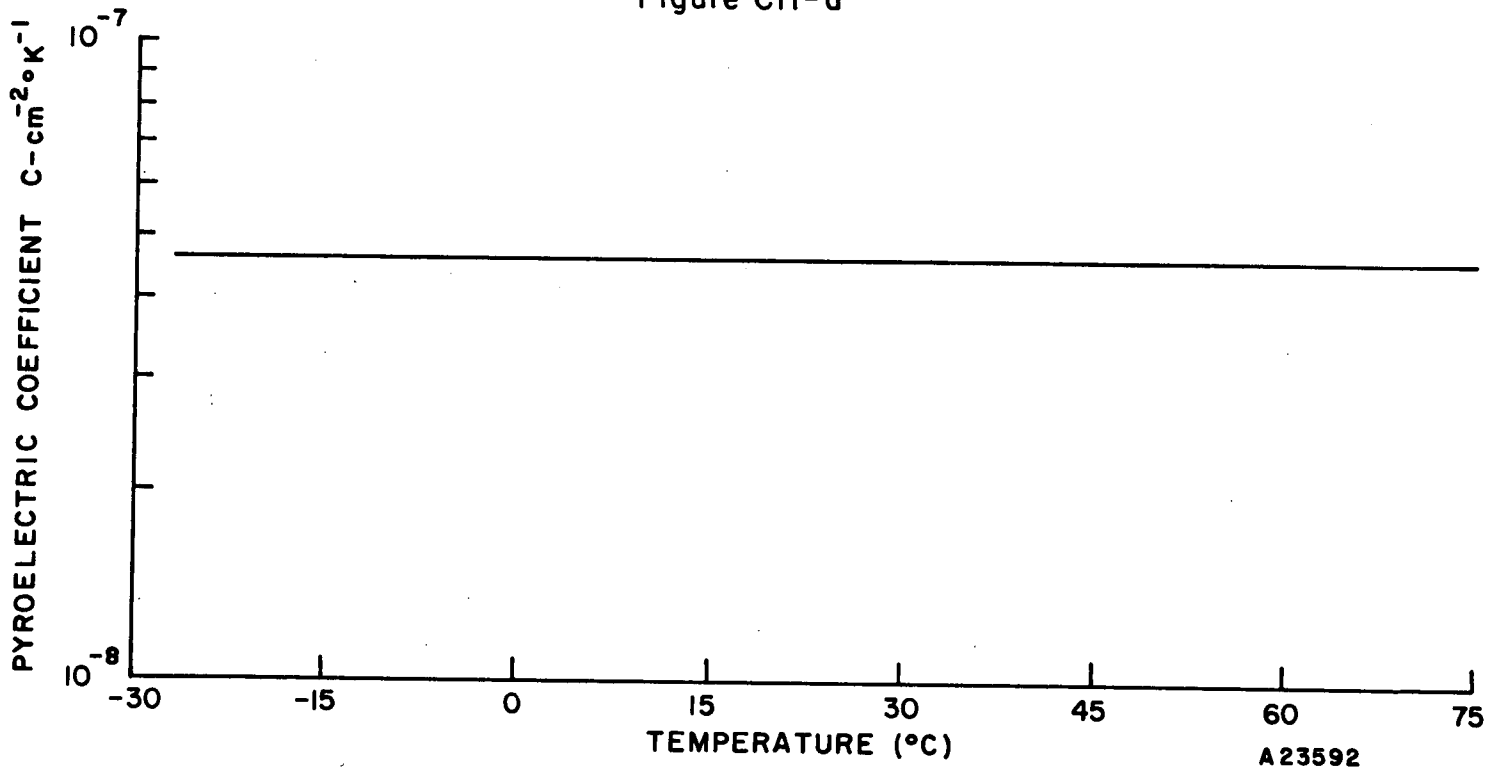
A23565

DIELECTRIC CONSTANT (ϵ_b)_{1KHz} & LOSS TANGENT OF
 $(Li_2O)_{0.49}(Ta_2O_5)_{0.51}$ VS. TEMPERATURE
 Figure C10-b



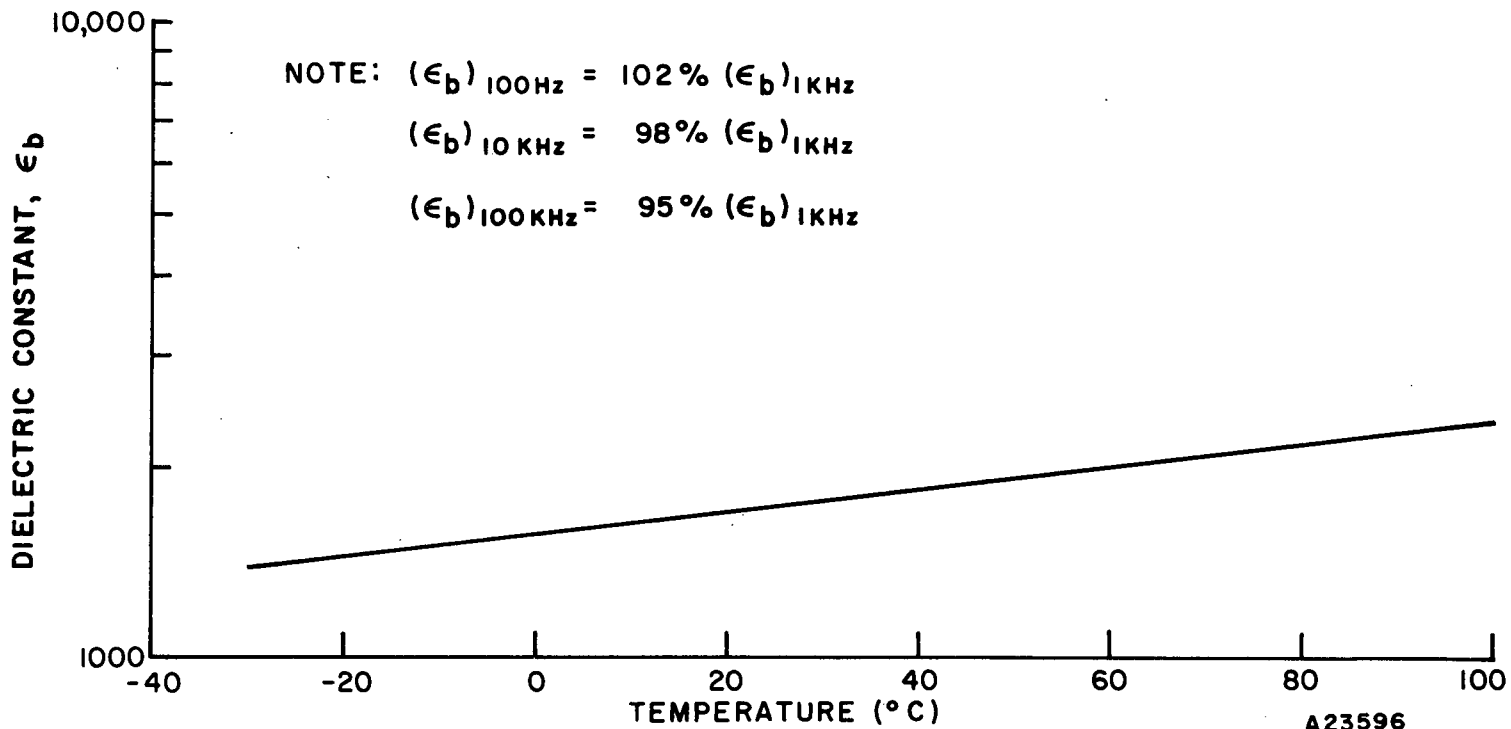
NOTE: ϵ_b AT 100Hz, 10KHz, 100KHz DEVIATED LESS THAN $\pm 0.5\%$ FROM INDICATED ϵ_b AT 1KHz OVER ENTIRE TEMPERATURE RANGE.

PYROELECTRIC COEFFICIENT OF GULTON PZT G-1306
VS. TEMPERATURE
Figure CII-a



A23592

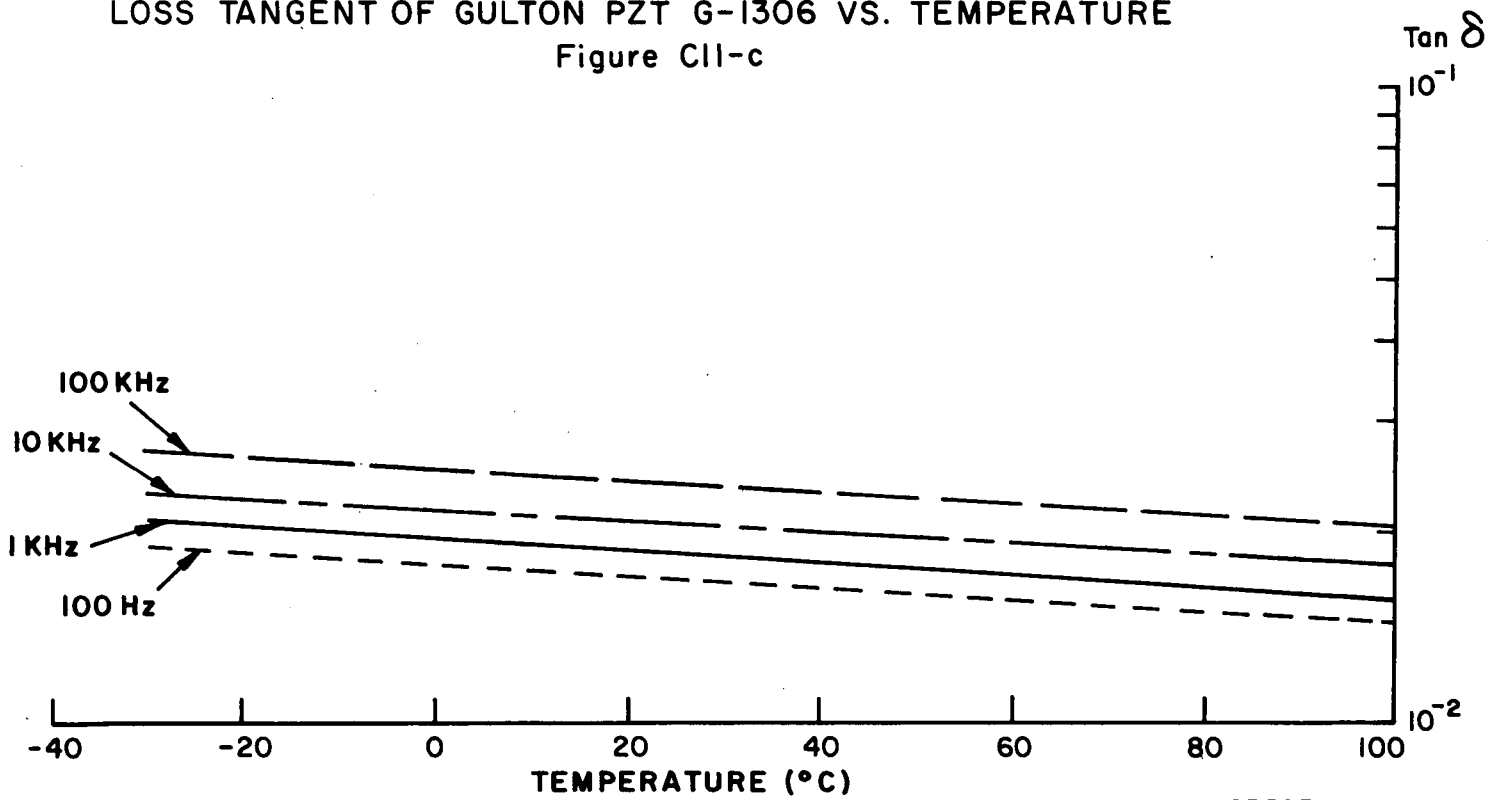
DIELECTRIC CONSTANT (ϵ_b)_{1KHz} OF GULTON PZT G-1306
VS. TEMPERATURE
Figure CII-b



A23596

LOSS TANGENT OF GULTON PZT G-1306 VS. TEMPERATURE

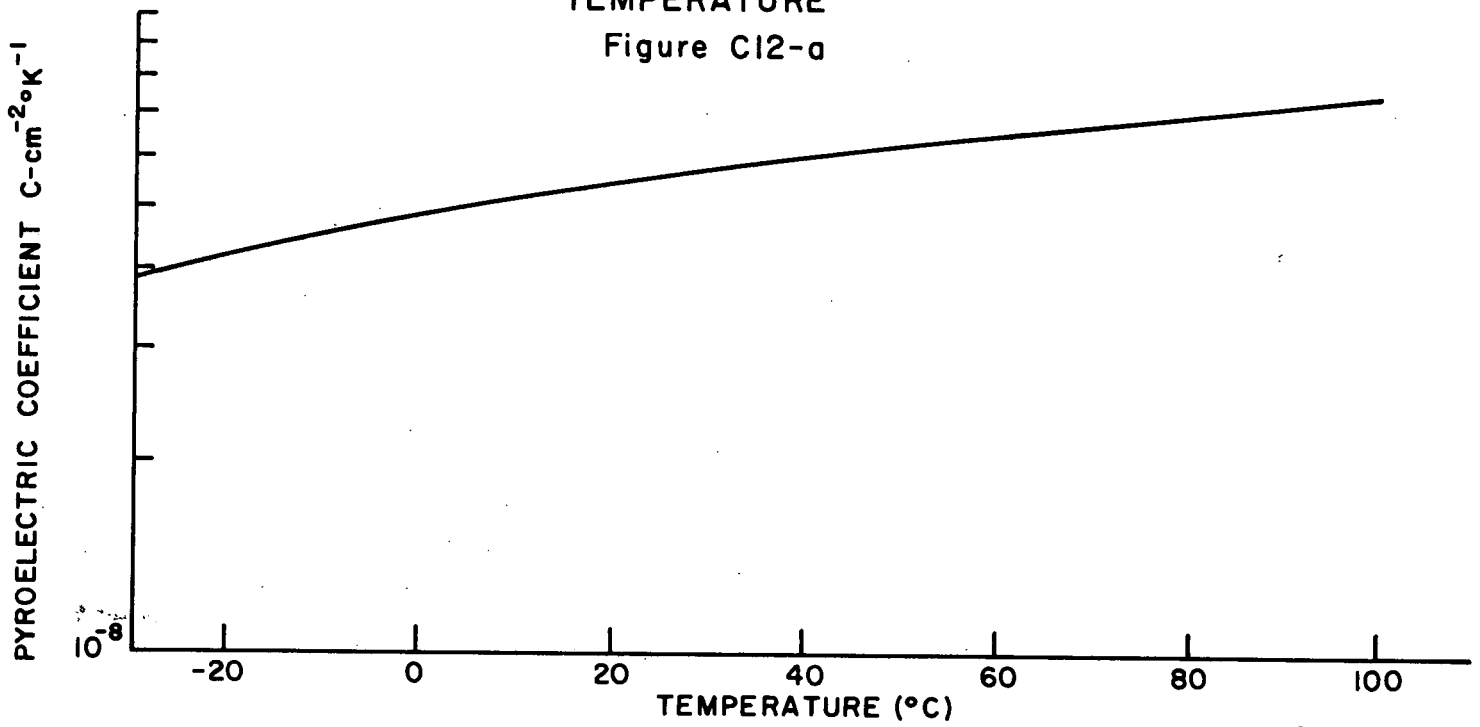
Figure CII-c



A23597

PYROELECTRIC COEFFICIENT OF HONEYWELL 4/60/40 PLZT VS.
TEMPERATURE

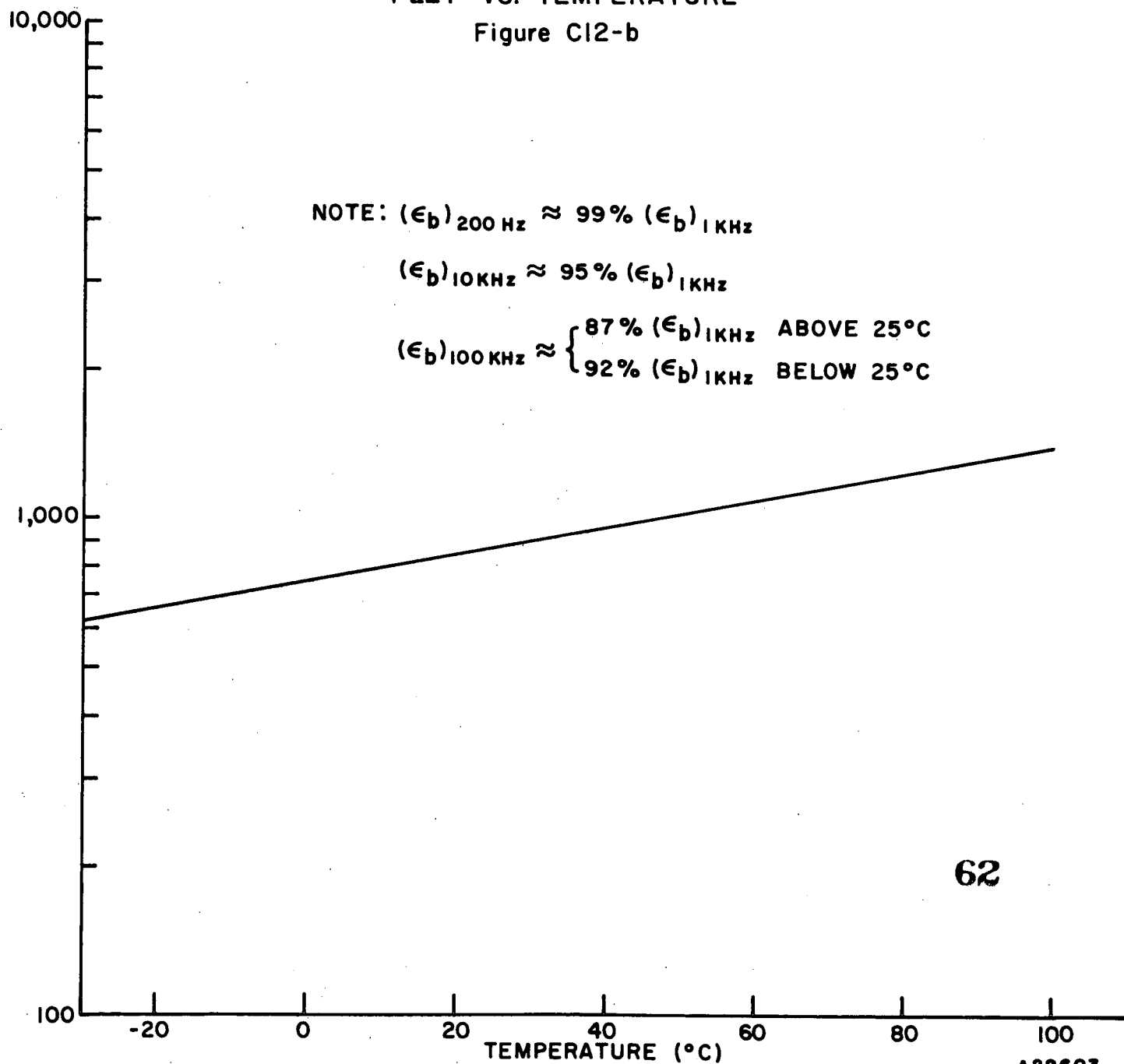
Figure C12-a



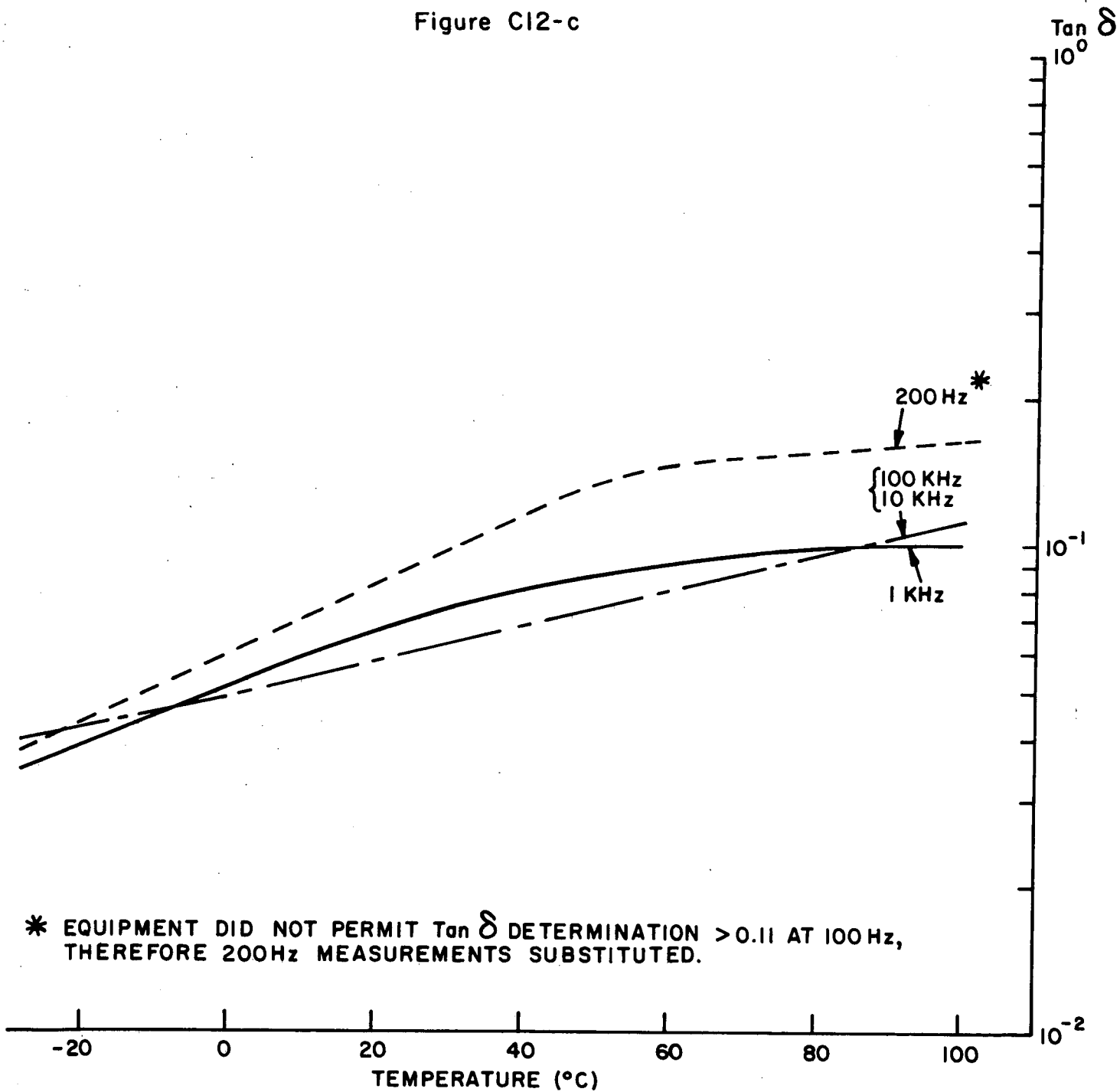
A23604

DIELECTRIC CONSTANT $(\epsilon_b)_{1Kc}$ OF HONEYWELL 4/60/40
PLZT VS. TEMPERATURE

Figure C12-b



LOSS TANGENT OF HONEYWELL 4/60/40 PLZT VS. TEMPERATURE
Figure C12-c

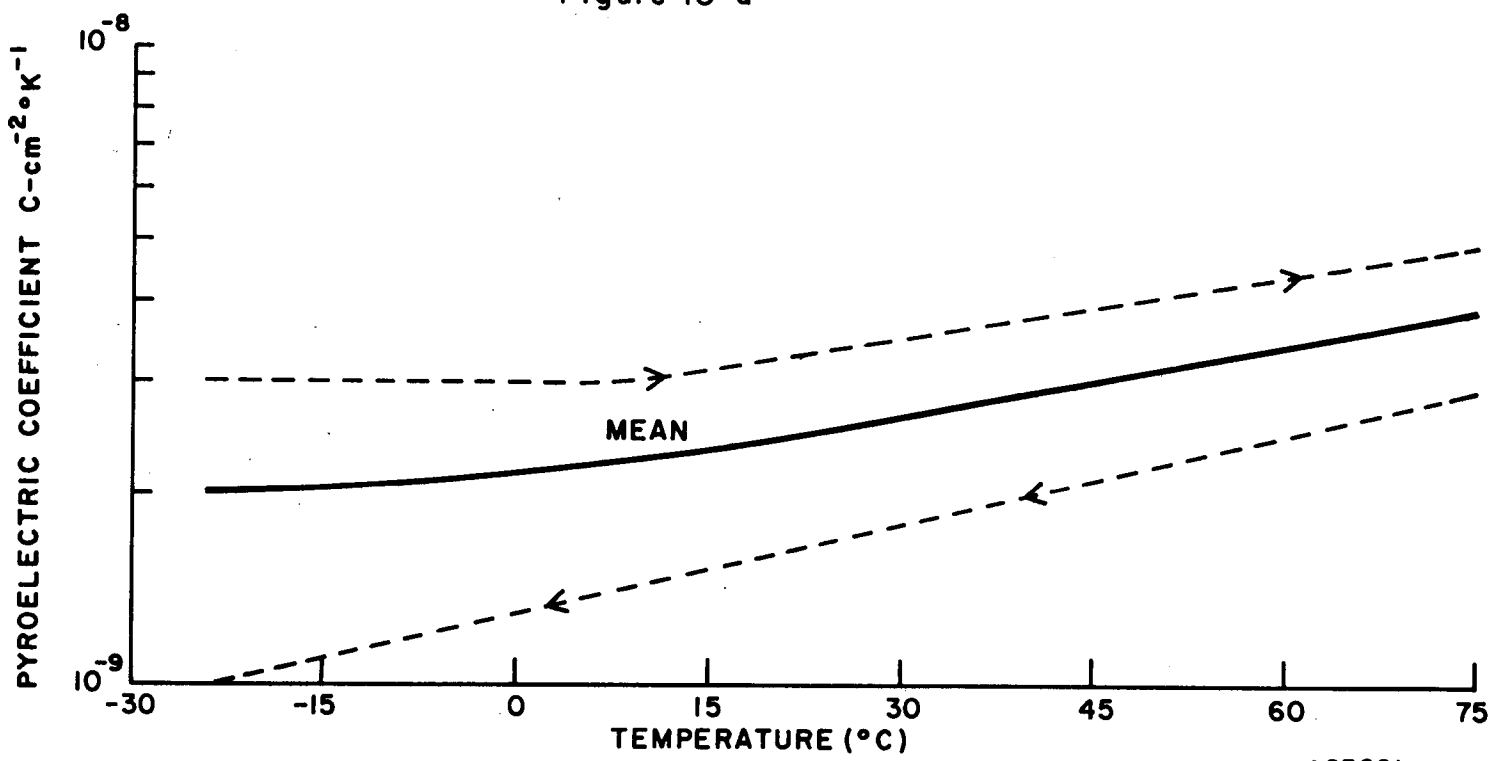


* EQUIPMENT DID NOT PERMIT Tan δ DETERMINATION > 0.11 AT 100 Hz, THEREFORE 200Hz MEASUREMENTS SUBSTITUTED.

A23605

PYROELECTRIC COEFFICIENT OF ETHYLENE DIAMINE
TARTRATE VS. TEMPERATURE

Figure 13-a



A23601

DISTRIBUTION LIST

<u>No. of Copies</u>	<u>Addressee</u>	<u>Code</u>
1	Systems Reliability Directorate	300
1	T & DS Directorate	500
1	Patent Counsel	204
1	Documentation Branch	256
1	GSFC Library	252
1	Contracting Officer	245
1	Space Sciences Directorate	600
3	Technical Officer	652